A simulation analysis of the fate of phytoplankton within the Mid-Atlantic Bight

by

John J. Walsh, Dwight A. Dieterle, and Mark B. Meyers

Department of Marine Science

University of South Florida

St. Petersburg, Florida 33701

ABSTRACT

A time-dependent, three-dimensional simulation model of wind-induced changes of the circulation field, of light and nutrient regulation of photosynthesis, of vertical mixing as well as algal sinking, and of herbivore grazing stress, is used to analyze the seasonal production, consumption, and transport of the spring bloom within the mid-Atlantic Bight. Our case (c) of a 58-day period in February-April 1979, simulated primary production, based on both nitrate and recycled nitrogen, with a mean of 0.62 g C m^{-2} day^{-1} over the whole model domain, and an export at the shelf-break off Long Island of 2.60 g chl m^{-2} day^{-1} within the lower third of the water column. About 57% of the carbon fixation was removed by herbivores, with 21% lost as export, either downshelf or offshore to slope waters, after the first 58 days of the spring bloom. Extension of the model for another 22 days of case (c) increased the mean export to 27%, while variation of the model's parameters in 8 other cases led to a range in export from 8% to 38% of the average primary production. Spatial and temporal variations of the simulated algal biomass, left behind in the shelf water column, reproduced chlorophyll fields sensed by satellite, shipboard, and in situ instruments.

INTRODUCTION

Satellite time series of the 1979 spring bloom within the mid-Atlantic Bight (WALSH, DIETERLE and ESAIAS, 1987a) and moored fluorometer time series of the 1984 spring bloom in the same region (WALSH, WIRICK, PIETRAFESA, WHITLEDGE, HOGE and SWIFT, 1987b) suggested that the daily export of algal biomass to slope waters might be 1.8-2.7 g chl m^{-2} day^{-1} across the shelf-break. Such time series lacked depth resolution, however, since the CZCS sampled, at most, the upper 10 m of the water column and the in situ instruments sampled perhaps the lower 5 m at the 80 m and 120 m isobaths. Furthermore, the algal biomass detected by the CZCS over space and by the moored fluorometer over time only represented what was left behind in the water column by the bacteria, zooplankton, and benthos of this shelf ecosystem.

To place these daily estimates of export in the context of seasonal production, consumption, and transport of the spring bloom, a simulation model of the plankton dynamics, over 6000 grid points in the horizontal plane and 3 depth layers in the vertical, was run for 58 days from 28 February to 27 April 1979 in response to wind-induced changes of the barotropic circulation field. The details of the time-dependent terms for the physical circulation, for the light and nutrient regulation of photosynthesis, for the vertical mixing, for the algal sinking, and for the grazing stress at ~18000 grid points are discussed below.

During the 6 yr interval between these CZCS and fluorometer time series, a set of biochemical surveys was also conducted each April aboard the R/V Kelez, Advance II, and Cape Henlopen. The April

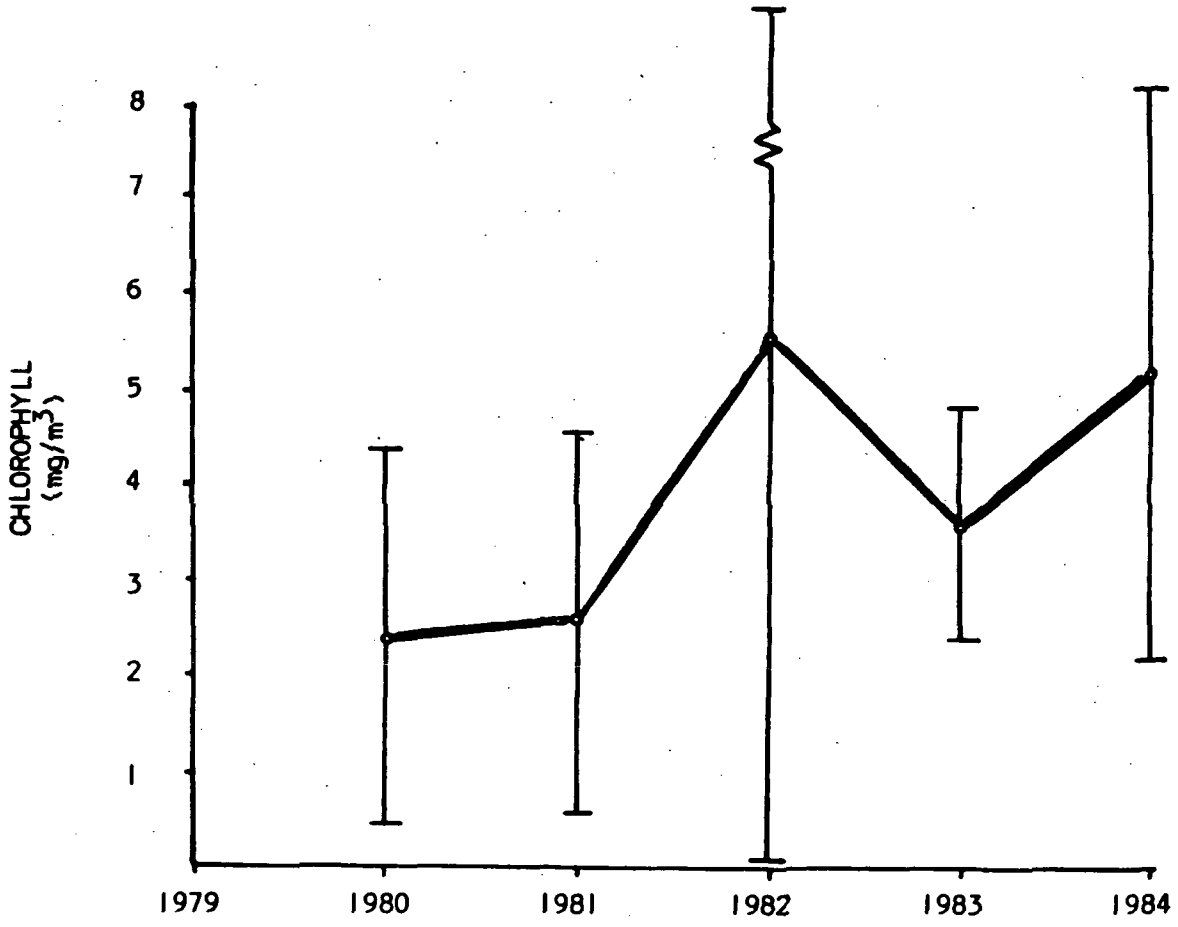

Figure 1. The mean chlorophyll content (mg m^{-3}) of surface waters (0-30 m) of the mid-Atlantic Bight at 27 stations re-occupied each April from 1980 to 1984 (W. GREGG, personal communication).

1980-84 chlorophyll content over the first attenuation depth (37% light level) at the same 27 station locations in estuarine (<20 m), shelf (20-200 m), and slope (>200 m) regions of the mid-Atlantic Bight is plotted (W. GREGG, personal communication) as Figure 1. The mean chlorophyll content of these waters may have doubled over 5 yr, from 2.38 μg chl ℓ^{-1} in April 1980 to 5.25 μg chl ℓ^{-1} in April 1984. Not surprisingly, the chlorophyll content of slope waters was the same each April, with the possible increase of algal biomass taking place in shelf and estuarine waters.

In contrast to pristine river contents of ~5-10 μg-at N ℓ^{-1} (WALSH, 1984), the dissolved nitrogen content at the freshwater end of the Hudson, Delaware, and Susquehanna estuaries was >50 μg-at N ℓ^{-1} in 1980 and may still be increasing as a result of sewage wastes and agricultural leachate. The volume of these estuaries, and thus the residence time for algal uptake of dissolved nitrogen, increases southward, with consequent export to the adjacent shelf of mainly dissolved nitrogen from the Hudson River plume and of mainly particulate nitrogen from the Chesapeake Bay plume (Fig. 2).

Most of the chlorophyll in Chesapeake Bay occurs upstream of the 25‰ isopleth of salinity, while most of the algal biomass in the Hudson River system is produced downstream of this isopleth (Fig. 2). At the 20 m isobath, seaward of the Hudson River estuary, tenfold more nitrate is thus present during the spring bloom than at the same depth off Delaware or Chesapeake Bay (Fig. 3). An assessment of the estuarine contribution to algal export at the shelf-break was also examined in the simulation model by altering the boundary flux of

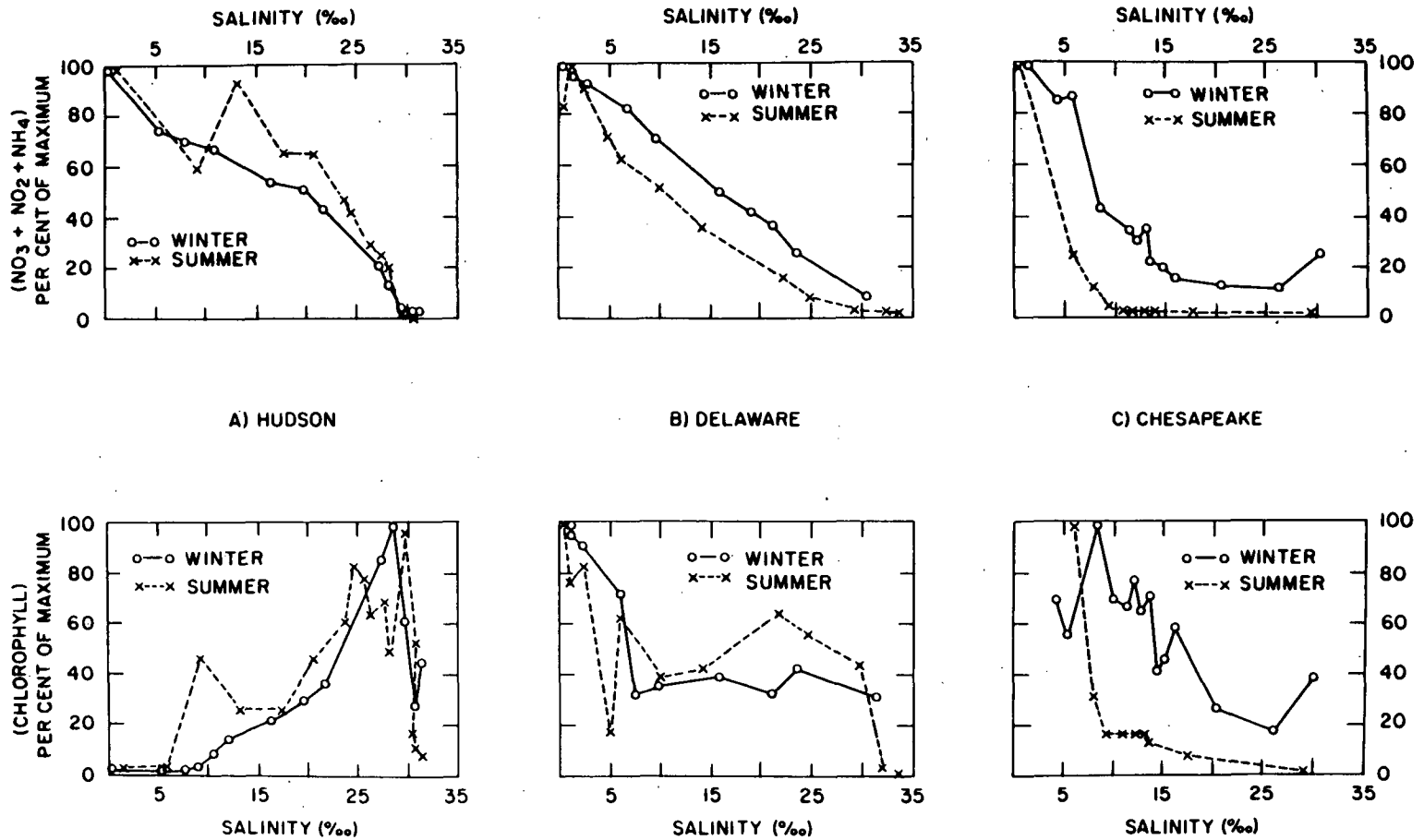

Figure 2. The nitrate and chlorophyll distributions within the a) Hudson, b) Delaware, and c) Chesapeake estuaries as a percentage function of their maximum value and salinity during winter (o) and summer (x) - after CARPENTER et al., 1969; McCARTHY et al., 1977; DECK, 1981; and SHARP et al., 1982.

nutrients at the mouths of these three estuaries as well as that from Long Island Sound (Fig. 4).

METHODS

1. Circulation

Ignoring tidal forces and the horizontal stress terms of the Navier-Stokes equations, their cross-differentiation and the continuity equation leads to a steady-state, depth-integrated form of the vorticity equation as

$$\left(\frac{\partial H}{\partial x}\frac{\partial \phi}{\partial y} - \frac{\partial H}{\partial y}\frac{\partial \phi}{\partial x}\right) + \left(\frac{\partial B_y}{\partial x} - \frac{\partial B_x}{\partial y}\right) - \left(\frac{\partial F_y}{\partial x} - \frac{\partial F_x}{\partial y}\right) = 0 \qquad (1)$$

where the first term is a description of vortex shrinking or stretching as a water parcel crosses an isobath, in which H is the bottom depth, and ϕ is the sea level potential, defined as the product of the acceleration of gravity and the height of the free surface elevation. The second and third terms are respectively the curl of the components of the bottom stress, B_y and B_x, and of the wind forcing, F_y and F_x in a left-hand cartesian coordinate system, with z positive downwards.

The bottom stress can be defined (HOPKINS and DIETERLE, 1983) in terms of the sea level potential and the wind stress by

$$B_x = a_1 \frac{\partial \phi}{\partial x} - a_2 \frac{\partial \phi}{\partial y} + b_1 \qquad (2)$$

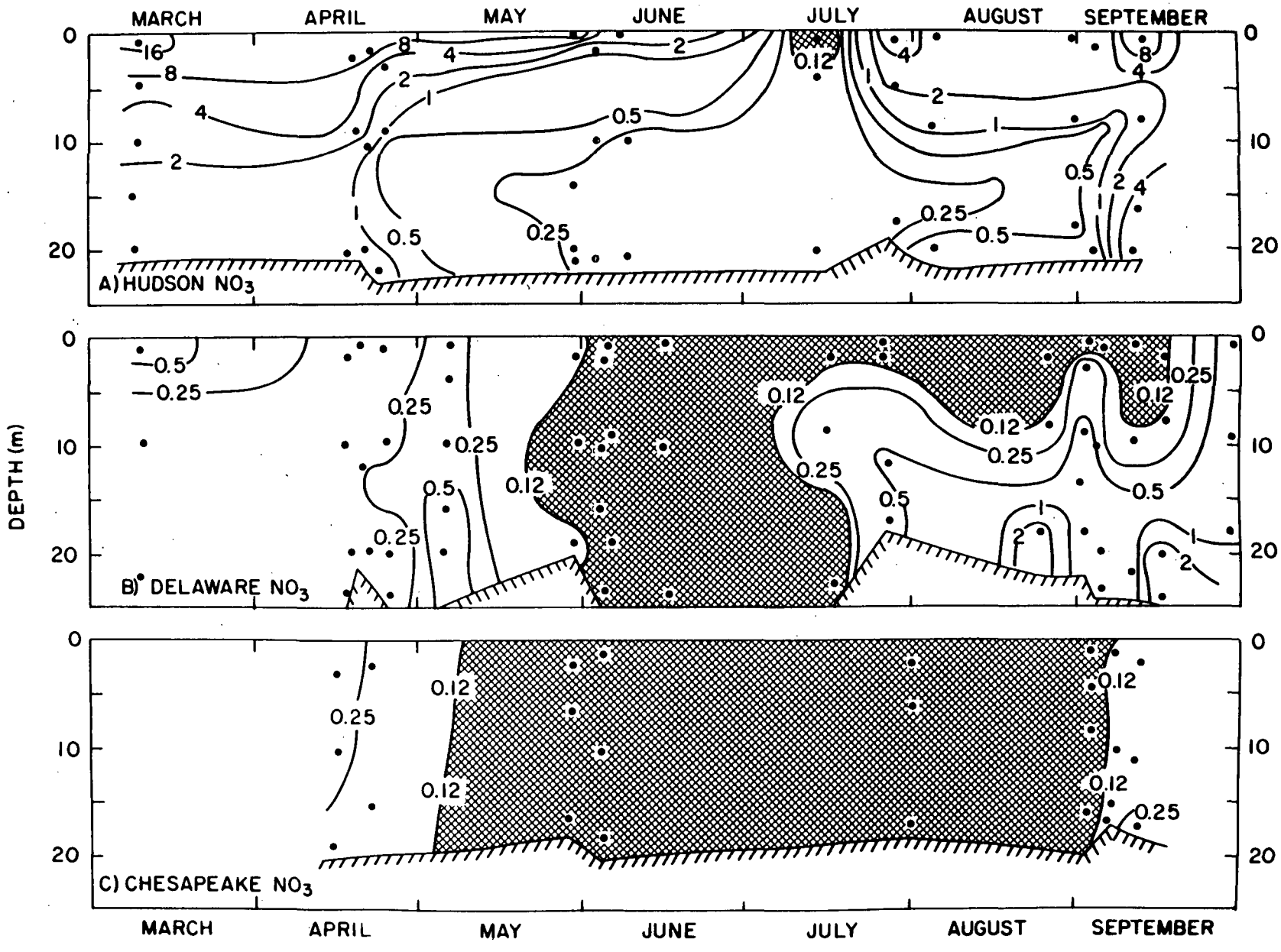

Figure 3. The seasonal structure of nitrate (μg-at ℓ^{-1}) at the 20 m isobath off the a) Hudson, b) Delaware, and c) Chesapeake estuaries during March-September (T. WHITLEDGE, personal communication).

$$B_y = a_2 \frac{\partial \phi}{\partial x} + a_1 \frac{\partial \phi}{\partial y} + b_2 \qquad (3)$$

where b_1 and b_2 represent that portion of the bottom stress due to the wind-driven velocity components. In waters deeper than the surface Ekman layer ($H \geq 30$ m), the bottom stress terms become similar to those of HSUEH and PENG (1978), e.g.,

$$B_y = \alpha \, (\cos \theta) \frac{\partial \phi}{\partial x} + \alpha \, (\sin \theta) \frac{\partial \phi}{\partial y} \qquad (4)$$

where θ is a bottom veer angle, and α represents a scaling depth. It is somewhat analogous to the depth of the bottom Ekman layer, in which α might be 5-15 m, with θ ranging from 0° to 45° (HSUEH and PENG, 1978; HSUEH, 1980; HAN, HANSEN and GALT, 1980; and CSANADY, 1981).

Substituting eqs. (2) and (3) in eq. (1), assuming that the wind curl is negligible, and setting $h = H + a_1$, leads to

$$\left(\frac{\partial h}{\partial x} \frac{\partial \phi}{\partial y} - \frac{\partial h}{\partial y} \frac{\partial \phi}{\partial x}\right) + a_2 \left(\frac{\partial^2 \phi}{\partial x^2} + \frac{\partial^2 \phi}{\partial y^2}\right) + \left(\frac{\partial a_2}{\partial y} \frac{\partial \phi}{\partial y} + \frac{\partial a_2}{\partial x} \frac{\partial \phi}{\partial y}\right) =$$

$$\left(\frac{\partial b_1}{\partial y} - \frac{\partial b_2}{\partial x}\right) \qquad (5)$$

which can be solved as a steady-state, boundary-value problem for the sea level potential.

Wind forcing also enters the solution of eq. (5), at the coastal boundary condition, where the depth-integrated transport normal to the

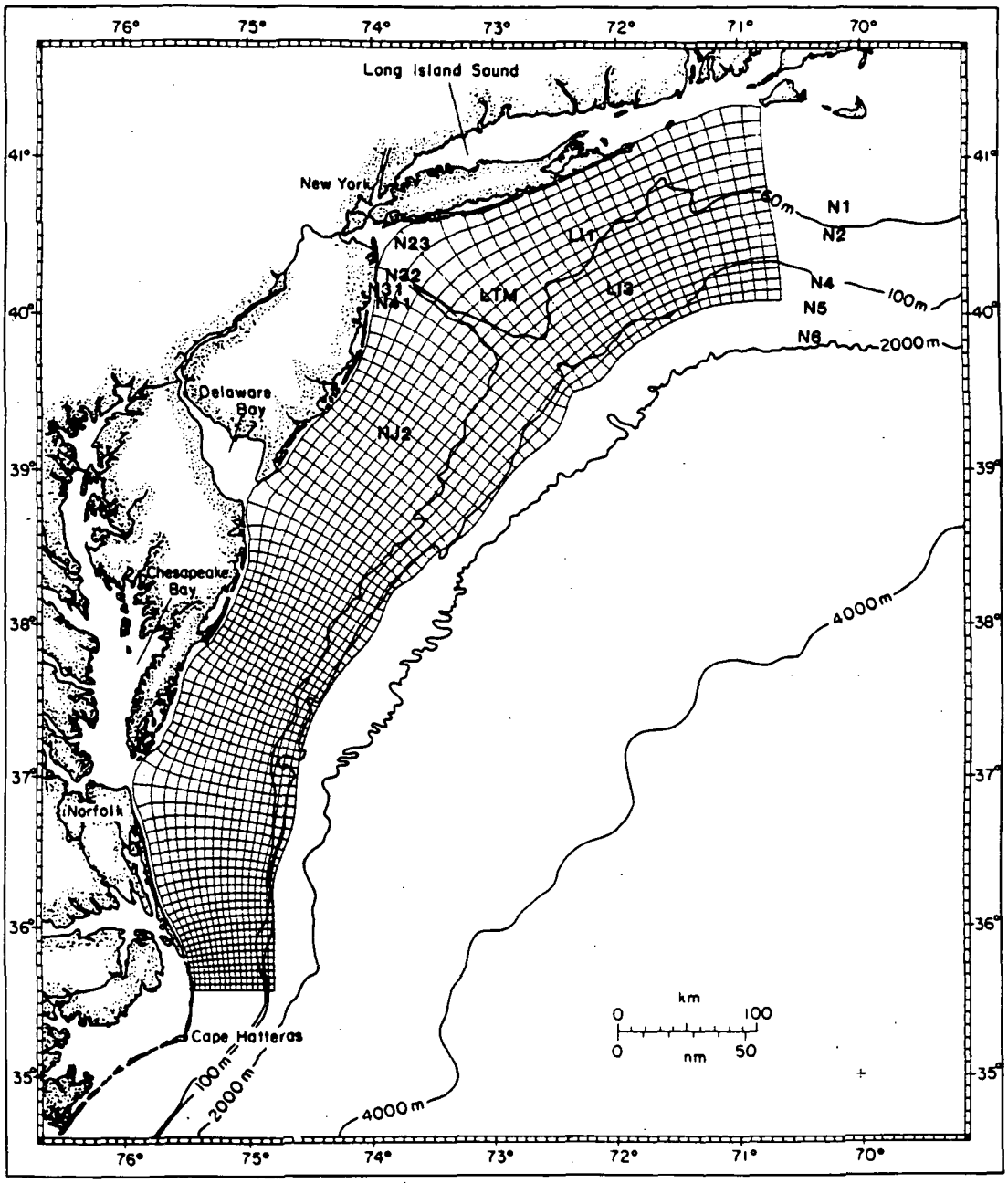

Figure 4. A 6,000 element curvilinear grid of a coupled physical-biochemical model of the mid-Atlantic Bight in relation to upstream (N1-N6) and interior (L11, L13, LTM, N23, N22, N31, N41, and NJ2) current meter moorings.

coastline, $U = \int_o^H u dz$, is assumed to be zero, except at the mouths of the three estuaries. The alongshore transport, $V = \int_o^H v dz$, at the coastal boundary (Fig. 4) is governed by the depth-integrated shallow water equation

$$\frac{\partial V}{\partial t} = - H \frac{\partial \phi}{\partial y} + F_y - B_y - fU \qquad (6)$$

where all the terms are defined above. At steady-state, i.e., $\frac{\partial V}{\partial t} = 0$, eq. (6) becomes

$$F_y = B_y + H \frac{\partial \phi}{\partial y} \qquad (7)$$

except at the estuaries, where U is non-zero. Use of eq. (3) results in

$$F_y = h \frac{\partial \phi}{\partial y} + a_2 \frac{\partial \phi}{\partial x} + b_2 \qquad (8)$$

at $x = 0$. For 13 time intervals between 28 February and 27 April 1979, the alongshore component of the mean wind stress observed at John F. Kennedy airport (Fig. 5) was entered in the simulation, with a new steady-state solution of ϕ calculated (HOPKINS and DIETERLE, 1983) at each grid point (Fig. 4) from a finite difference form of eqs. (5) and (8).

The open water boundary conditions for ϕ must also be specified, of course, for solution of this boundary value problem. The sea

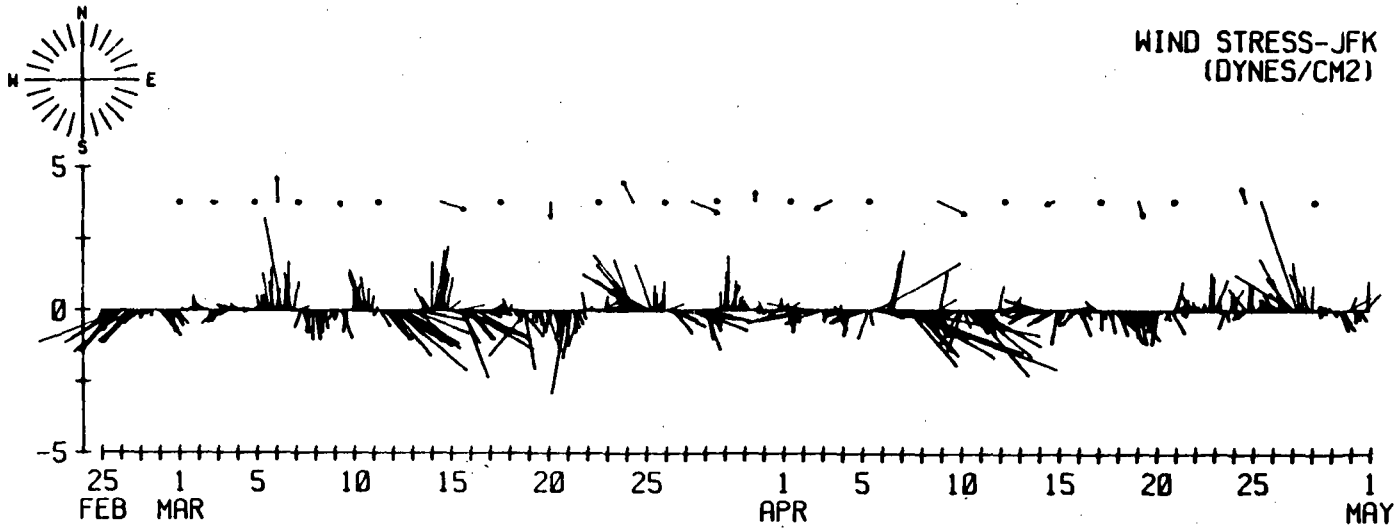

Figure 5. The daily and mean wind stress (dynes cm^{-2}) over 13 periods as measured at the John F. Kennedy airport between 25 February and 1 May 1979.

elevation at the upstream boundary of the grid was computed from the observed currents (BEARDSLEY, CHAPMAN, BRINK, RAMP and SCHLITZ, 1985) at N1 to N5 (Fig. 4) for each time interval (Fig. 5). Since the April 1979 currents were mainly barotropic in the mid-Atlantic Bight (HOPKINS and DIETERLE, 1987) and hydrographic data on density gradients were sparse, we did not attempt to subtract the baroclinic component of flow from the current meter records. At the offshore boundary, sea elevation was set to a constant 5 cm, i.e., mass exchange was confined at the shelf-break to the surface and bottom Ekman layers. At the downstream boundary (Fig. 4), $\frac{\partial^2 \phi}{\partial y^2} = 0$ was specified (HSUEH, 1980).

At each point of the curvilinear grid (HOPKINS and DIETERLE, 1983) of the model, i.e., a length of 886 km alongshore at the coast and 676 km at the shelf-break (Fig. 4), ϕ was first computed for each of the 13 wind cases and then inserted in the steady-state Ekman equations

$$\frac{\partial \phi}{\partial x} = K_z \frac{\partial^2 u}{\partial z^2} + fv \tag{9}$$

$$\frac{\partial \phi}{\partial y} = K_z \frac{\partial^2 v}{\partial z^2} - fu \tag{10}$$

for evaluation of u and v. Analytical solution of eqs. (9) and (10) then allowed (HOPKINS and SLATEST, 1986) continuous depth resolution of the flow field for different values of the wind stress and vertical eddy diffusivity, K_z, at each steady state. In the biochemical

calculation of eqs. (11) and (12), u and v were entered as the mean of their depth integral over each of three vertical layers, where the depth, Z, of a layer varied across the shelf as a function of the bottom depth, H, i.e., Z = H/3.

2. Light and nutrient regulation

The spatio-temporal distributions of nitrate (N) and chlorophyll (M) were calculated from

$$\frac{\partial N}{\partial t} = - u \frac{\partial N}{\partial x} - v \frac{\partial N}{\partial y} - w \frac{\partial N}{\partial z} + K_z \frac{\partial^2 N}{\partial z^2} - b\varepsilon M \qquad (11)$$

$$\frac{\partial M}{\partial t} = - u \frac{\partial M}{\partial x} - v \frac{\partial M}{\partial y} - w \frac{\partial M}{\partial z} + K_z \frac{\partial^2 M}{\partial z^2} + \varepsilon M - w_s \frac{\partial M}{\partial z} - gM \qquad (12)$$

where u and v are the horizontal velocities, w is the vertical velocity derived from the continuity equation, K_z is the vertical eddy or mixing coefficient discussed below, b is the nitrate/chlorophyll ratio of 0.5, ε is the phytoplankton growth rate described in this section, w_s is the sinking rate of the phytoplankton, and g is the grazing loss rate to herbivores.

In this simulation analysis, we were concerned with the amount of phytoplankton export from the mid-Atlantic shelf, which depends on the amount of "new" dissolved nitrogen added from the slope and estuarine boundaries (EPPLEY and PETERSON, 1980; WALSH, 1981), not the recycled production based on ammonium or urea regenerated within the shelf

ecosystem. We thus did not consider the growth of phytoplankton in eq. (12) from excretory products (WALSH, 1975), implicit within the grazing loss term.

The input of nitrate from the coastal boundary was assumed to be 10.0 μg-at NO_3 ℓ^{-1} from the Hudson River, 1.3 μg-at NO_3 ℓ^{-1} from Chesapeake Bay, 1.0 μg-at NO_3 ℓ^{-1} from Delaware Bay, and 1.0 μg-at NO_3 ℓ^{-1} from Long Island Sound. Most of the model's cases assumed that the nitrate boundary condition of slope water and of upstream shelf water was 6.0 μg-at NO_3 ℓ^{-1} throughout the water column. The estuarine boundary conditions of nitrate were later increased tenfold for the eutrophication case, while in two simulation runs the upstream nitrate content was set instead to 1.0 μg-at NO_3 ℓ^{-1}.

The specific growth rate (hr^{-1}) of the phytoplankton, ε, was a function of ambient light (I) and nitrate (N)

$$\varepsilon = \varepsilon_m [I/I_s e^{(1 - I/I_s)}][\frac{N}{n + N}] \qquad (13)$$

where ε_m was the maximum growth rate of 0.026 hr^{-1}, assuming a mean temperature of 5°C and a phytoplankton assemblage of 50% netplankton (MALONE, 1982). The saturation light intensity, I_s, of STEELE's (1962) inhibition expression was taken to be 5 cal cm^{-2} hr^{-1} (MALONE, 1977). The Michaelis half-saturation constant, n, of the nutrient limitation term (CAPERON, 1967), at which $\varepsilon = \varepsilon_m/2$, was taken to be 1 μg-at NO_3 ℓ^{-1} for coastal phytoplankton species (CARPENTER and GUILLARD, 1971). The depth integral of ambient light over each of the 3 layers was actually a time-dependent function of season, day length, diel periodicity, and algal biomass.

Such a complex light field was described by

$$I(z,D,t) = \delta I_m \sin^3 [\pi(t - a)/i(D)] e^{-(k_w + k_s)z - k_p \int_o^Z Mdz} \quad (14)$$

where the seasonal light variation in the model was first described (NAGLE, 1978) as a cosine function of incident radiation (I_o) at the winter solstice, I_o^W (120 g cal cm^{-2} day^{-1}), at the summer solstice, I_o^S (500 g cal cm^{-2} day^{-1}), and the Julian date, D, of the 58-day simulation,

$$I_o(D) = I_o^W + 0.5(I_o^S - I_o^W)[1 - \cos 2\pi(D - 356)/365] \quad (15)$$

The changing photoperiod, or day length, was similarly described by

$$i(D) = i^W + 0.5(i^S - i^W)[1 - \cos 2\pi(D - 356)/365] \quad (16)$$

where i^W = 9.1 hr and i^S = 15.6 hr (NAGLE, 1978). The photosynthetically active radiation (PAR) at depth is about 50%, of which 15% might be lost as a result of albedo, such that δ was taken to be 0.425 in this model.

With specification of the day length, input of total radiation to the sea surface, and % transmission of 400-720 nm wavelengths, the hourly change of solar irradiance with time, t, can be expressed (IKUSHIMA, 1967) as

$$I_o(t) = I_m \sin^3[\pi(t - a)/i(D)] \quad (17)$$

where I_m is the maximum light intensity at local noon (g cal cm^{-2} hr^{-1}) for that Julian day, D, and a is the time of sunrise. The solar irradiance for the day is

$$I_o(D) = \int_o^{i(D)} I_m \sin^3[\pi(t - a)/i\,(D)]\, dt \quad (18)$$

and was used to obtain I_m in eq. (17), after solution of eqs. (15) and (16) for each simulated day of the model.

Finally, the integrated light field for algal photosynthesis over the depth interval, Z, was computed from the self-shading, exponential term of eq. (14), where the total extinction coefficient has been partitioned into those for water, k_w; detritus, k_s; and phytoplankton, k_p. The specific attenuation coefficient for plant pigments was assumed to be 0.020 m^2 mg^{-1} chl a (BANNISTER, 1974; JAMART, WINTER, BANSE, ANDERSON and LAM, 1977). The water and detrital contribution to water clarity, $k_w + k_s = 0.13$ m^{-1}, was derived as the average residual from the observed extinction coefficient and pigment concentration during 15-24 March 1979 (WALSH et al., 1987a).

Initial conditions of the spatial chlorophyll field of eqs. (11), (12), and (14) were obtained from a CZCS image of the mid-Atlantic Bight on 28 February 1979 (SYSTEMS AND APPLIED SCIENCES CORPORATION, 1984), at about the same spatial resolution as the model's grid (Fig. 4). The 1.0 μg ℓ^{-1} surface isopleth of chlorophyll was located

near the 20 m isobath, and the 0.5 μg ℓ^{-1} isopleth at the 60 m isobath, with the assumption of uniform pigment distribution within the 3 vertical layers of the model. The estuarine boundary conditions of algal biomass were respectively 7.5, 5.0, 4.0, and 3.0 μg chl ℓ^{-1} from the Hudson River, Delaware Bay, Long Island Sound, and Chesapeake Bay. The chlorophyll contents of inflowing shelf and slope waters were instead set to 0.5 and 0.2 μg chl ℓ^{-1} at the upstream and offshore boundaries.

Since Z was a function of the bottom depth, the upper layer of the model was 10 m deep at the 30 m isobath and 30 m deep at the 90 m isobath as a result of entering the known bottom topography, H, every ~3 km in the model. The observed depth of the euphotic zone in the mid-Atlantic Bight during March ranges, however, from about 10 m in the Hudson River plume (MALONE, HOPKINS, FALKOWSKI and WHITLEDGE, 1983) to ~30 m at the shelf-break (WALSH et al., 1987a). Thus a surface layer of variable depth (as well as the middle and bottom layers) in the model mimics fairly well the spatial changes of biological processes across the shelf.

3. Vertical mixing

Time series of CZCS images and vertical profiles of chlorophyll in March-April 1979 and 1984 (WALSH et al., 1987a; WALSH et al., 1987b) implied a downward displacement and/or sinking rate of 20-40 m day^{-1} for biogenic particles. Using a one-dimensional model (NIILER, 1975) of the wind-induced mixed layer, WROBLEWSKI and RICHMAN (1986) computed a vertical eddy coefficient, K_z, of 68 m^2 hr^{-1} (188 cm^2

sec^{-1}) over a 44 m deep mixed layer of weak vertical stratification (0.35 σ_t 50 m^{-1}), after 8.5 hr of a 10 m sec^{-1} wind forcing. The decay time for a return of K_z to 8 m^2 hr^{-1} (22 cm^2 sec^{-1}) was of the same order of 24 hr after cessation of the wind impulse.

During February-May 1979-82, a wind event ≧10 m sec^{-1} occurred about every 8 days in the mid-Atlantic Bight and at 27 shelf stations, during 16-24 March 1979, the vertical density gradient was a mean of 0.33 σ_t 52 m^{-1}. Over a 44 m surface mixed layer in the mid-Atlantic Bight, the equivalent vertical displacement rate from a K_z of 68 m^2 hr^{-1} would be 37.1 m day^{-1} during such March wind events. We wished to distinguish, however, between downwelling, i.e., w of eqs. (11) and (12), vertical mixing, i.e., K_z, and sinking of phytoplankton, i.e., w_s.

We thus computed (CSANADY, 1976) smaller values of K_z from

$$K_z = \frac{\tau\rho^{-1}}{200\ f} \tag{19}$$

for each of the wind cases (Fig. 5), where τ was the mean wind stress and ρ was the density of water. Values of K_z ranged in this model from 17 to 80 cm^2 sec^{-1}, i.e., at most about half of WROBLEWSKI and RICHMAN'S (1986) estimate, except for one run when all values of K_z were doubled. Each of the 13 values of K_z were entered both in eqs. (9) and (10) to compute u and v, and in eqs. (11) and (12) to compute vertical fluxes of nitrate and phytoplankton.

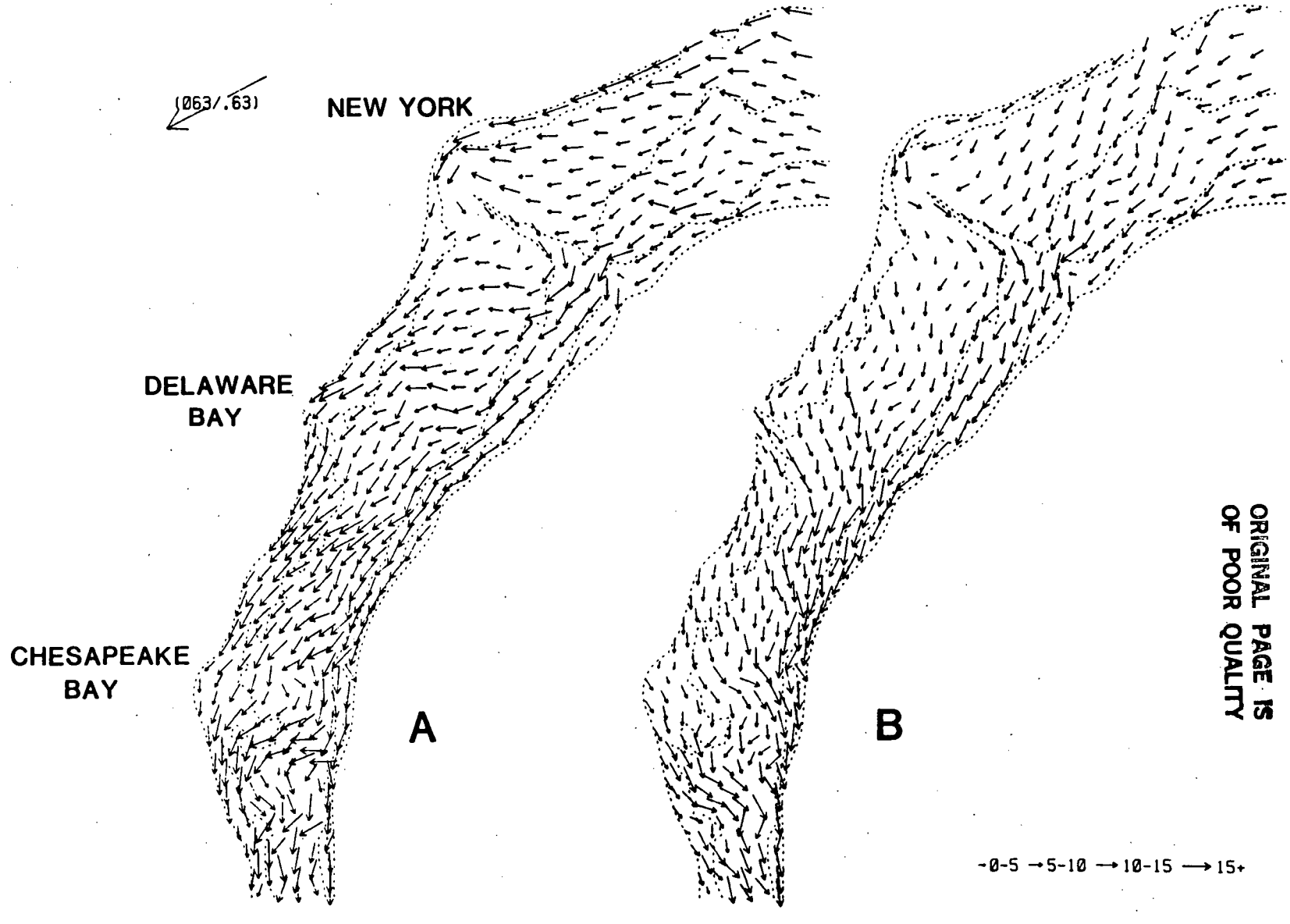

Figure 6. The simulated velocity fields (cm sec^{-1}) of the upper a) and lower b) thirds of the water column under a wind forcing of 0.63 dynes cm^{-2} from 063°T during 1-5 April 1979.

4. Sinking

Although laboratory sinking rates of diatoms range from only ~1 to 10 m day^{-1} (SMAYDA, 1970), repeated daily field observations of the 1975 diatom spring bloom at the 80 m isobath in the Baltic Sea indicated apparent sinking rates of 30 to 50 m day^{-1} (BODUNGEN, BROCKEL, SMETACEK and ZEITZSCHEL, 1981). Time series of stations taken ~2 days apart during the 1978-81 spring blooms in the southeastern Bering Sea suggested net in situ sinking rates at the 75 m isobath of only ~3-4 m day^{-1} (WALSH, 1983), but winds were favorable for upwelling about 50% of the time. Vertical chlorophyll profiles taken every 3 hours at the 70 m isobath off Long Island after a 15-20 m sec^{-1} wind event on 3-6 April 1975 again implied a range in sinking velocities of 12-50 m day^{-1} (WALSH, 1983). Within the present model, we employed a range in sinking rates of 0 to 20 m day^{-1} for w_s within the water column, at the sea surface, and at the water-sediment interface.

5. Grazing

Zooplankton grazing rates in the mid-Atlantic Bight during March are about 10% of the daily primary production (WALSH, WHITLEDGE, BARVENIK, WIRICK, HOWE, ESAIAS and SCOTT, 1978; DAGG and TURNER, 1982; SMITH and LANE, 1987), with an increase to ~40% by April (DAGG and TURNER, 1982; SMITH and LANE, 1987), and more than 100% by October (DAGG and TURNER, 1982). From March to April 1984, the dominant herbivore, Calanus finmarchicus, increased 8-fold in abundance over a 33-day period (SMITH and LANE, 1987), suggesting an exponential

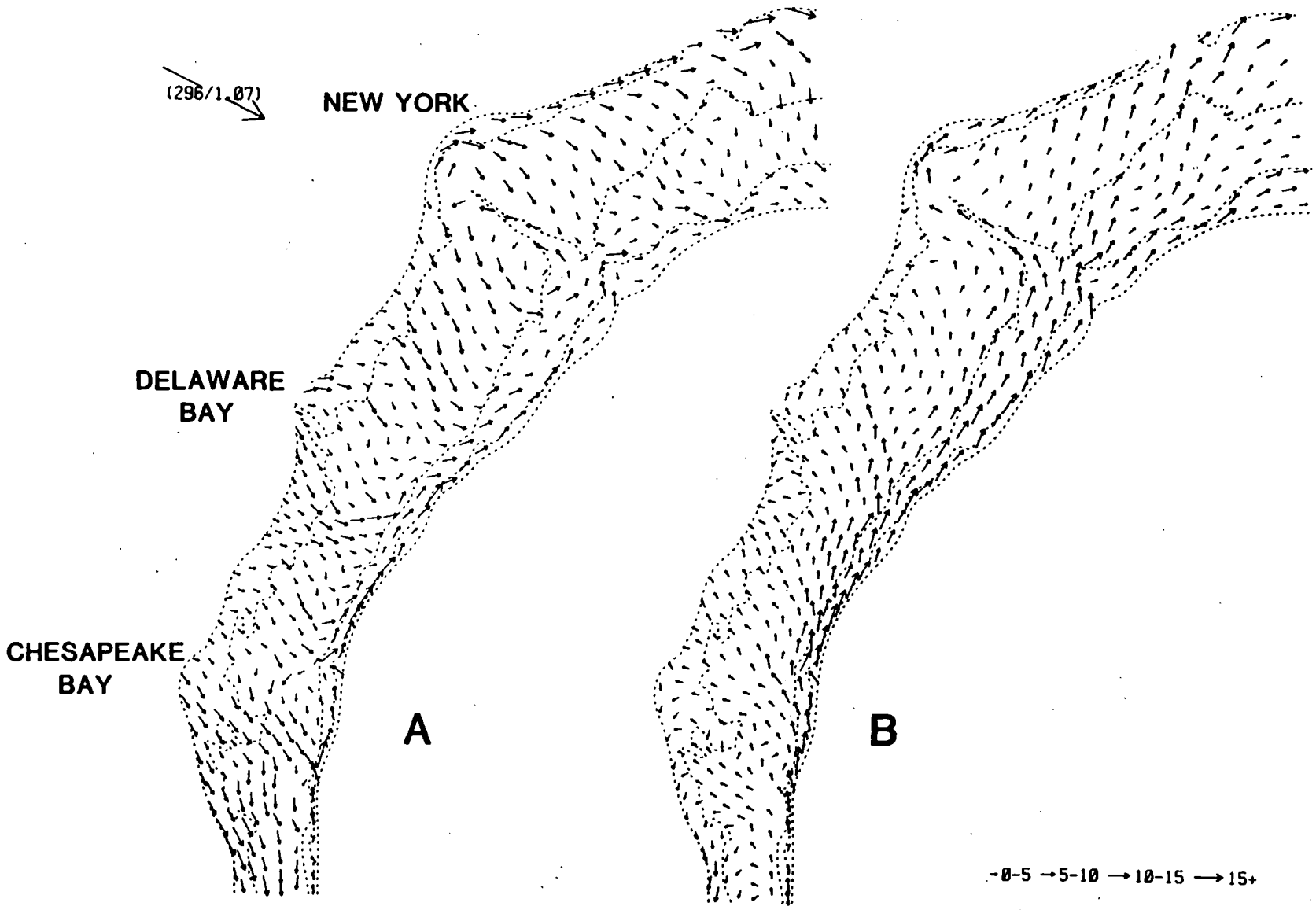

Figure 7. The simulated velocity fields (cm sec^{-1}) of the upper a) and lower b) thirds of the water column under a wind forcing of 1.07 dynes cm^{-2} from 296°T during 5-12 April 1979.

increase of this herbivore population, with a doubling time of about 10 days.

In this model, we thus mainly employed an exponential increase of the grazing stress, gM, from 28 February to 27 April by using

$$g = \ln(1 - G)/[24 - i(D)] \qquad (20)$$

where G was $0.03\ e^{-0.023(59 - D)}$ for H > 50 m, while G was a constant 0.06 for H < 50 m, i.e., there was a spatial gradient of grazing pressure. To simulate diurnal migration of the copepod grazers, this grazing stress was only imposed on the phytoplankton of the upper and middle layers of the model at night. In terms of primary production, the exponential grazing stress led to a loss of about 10% of the daily growth increment in February and 100% at the end of April, i.e., losses to benthos and bacterioplankton were then represented by this term as well. In one experiment of this model, no grazing stress was assumed, while in another experiment, a linear increase in grazing stress from March to April of $G = 0.1 + 0.0078(D - 69)$, for $D > 69$, was instead applied.

6. Computation

The circulation sub-model was solved by Gaussian elimination (EISENSTAT, SCHULTZ and SHERMAN, 1976), with the steady-state values of u, v, w, and K_z entered in eqs. (11) and (12) for the 13 time intervals (Fig. 5). Information about N and M was then obtained, not from deduction (CHRISTIE, 1941), but from numerical solution. The time-dependent solutions of the biochemical state equations were thus

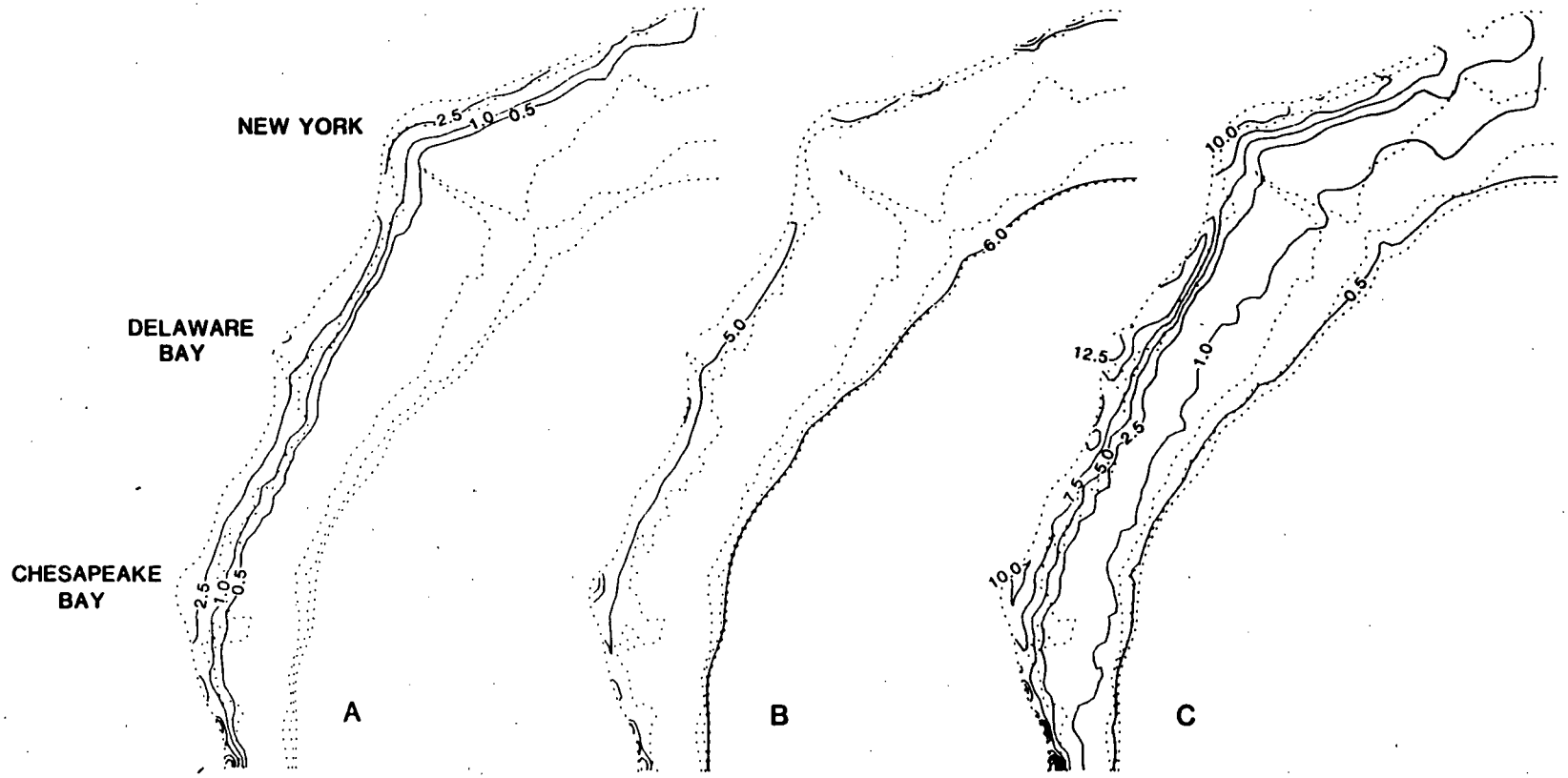

Figure 8. The simulated chlorophyll (μg ℓ^{-1}) of case (c) within the upper a) and lower c) layers, as well as nitrate (μg-at ℓ^{-1}) in b) the upper layer, on 3 March 1979.

obtained over a staggered grid of the same dimensions of the circulation model (Fig. 4), with an upstream or "donor cell" finite difference in space (ROACHE, 1976). Integration over time was done with a semi-implicit method for the vertical diffusion term and an explicit, forward in time, differencing method for the other terms (ROACHE, 1976).

RESULTS

The simulated flow fields of the circulation model were compared (WALSH et al., 1987a) with AOML current meter observations (MAYER, HAN and HANSEN, 1982) for April 1979 at 8 moorings in the New York Bight (Fig. 4). During this time period, the barotropic flow was about 90% of the transport, agreeing with a prior model's currents within a vector error of only ~1 cm sec^{-1} and 10° in the New York Bight (HOPKINS and DIETERLE, 1987). The extension of this circulation model to the mid-Atlantic Bight has been previously discussed (WALSH et al., 1987a), and yielded a mean difference between simulated and observed currents of 3 cm sec^{-1} velocity and 35° direction during 5-16 April 1979. The results of the biochemical calculations will thus be stressed in this analysis.

To provide perspective on the biological response to downwelling and upwelling events, however, the flow fields during 1-5 April (Fig. 6) and 5-12 April (Fig. 7) are shown for respective wind forcings of 0.63 dynes cm^{-2} from 063°T and 1.07 dynes cm^{-2} from 296°T (Fig. 5). The surface Ekman layer of the model exhibited onshore flows of 10-15 cm sec^{-1} (Fig. 6a) during the northeast wind forcing of 1-5 April, for example, while the bottom layer displayed similar

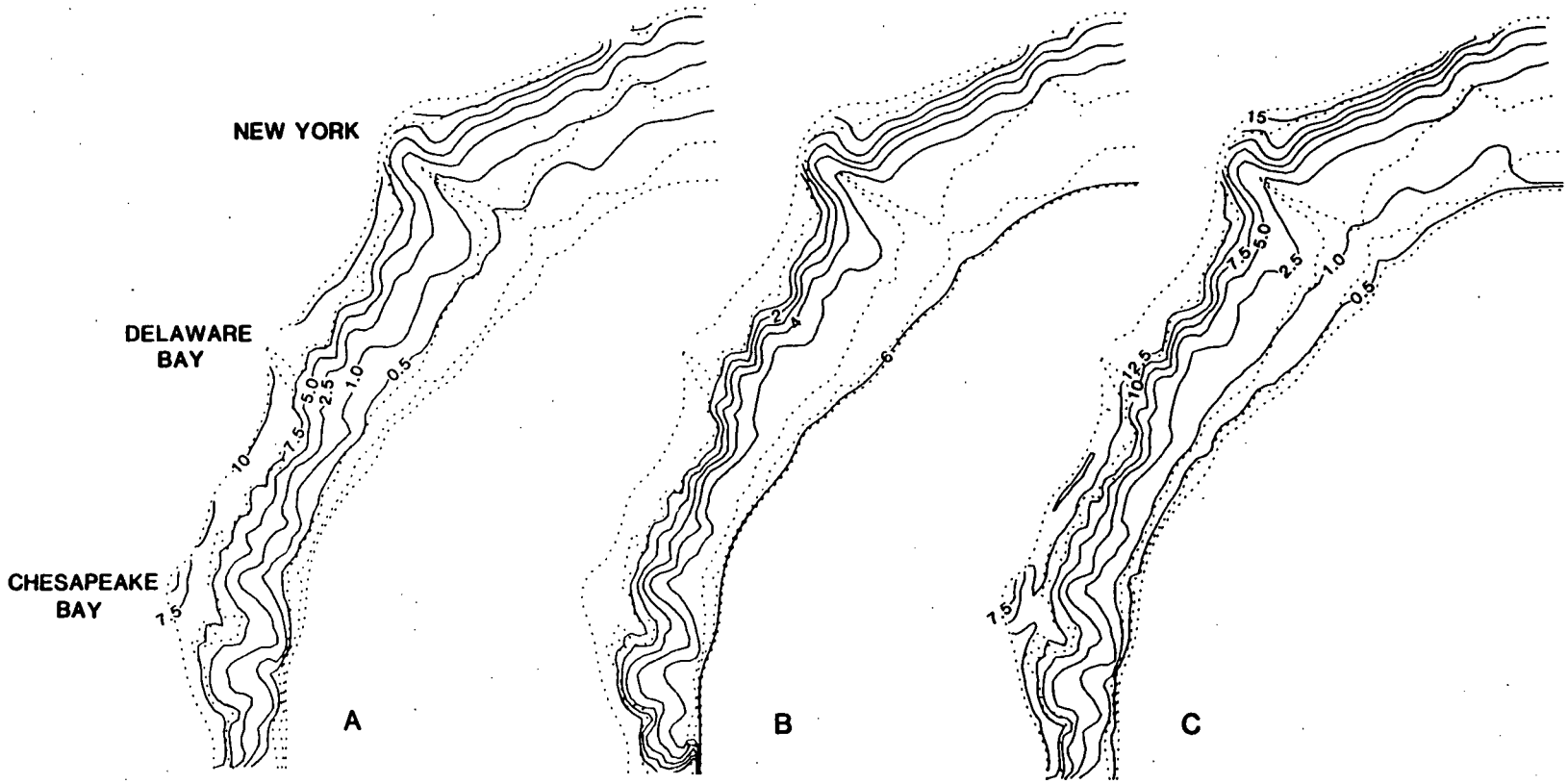

Figure 9. The same variables 13 days later on 16 March 1979.

offshore flow (Fig. 6b), particularly south of New Jersey. The vertical mixing coefficient was computed to be 42.7 cm^2 sec^{-1} during this time period, with maximum downwelling velocities of 23-26 m day^{-1} on the inner (<30 m depth) and middle (30-60 m depths) parts of the shelf.

With a shift in wind forcing to the northwest during 5-12 April, weaker offshore flows of 5-10 cm sec^{-1} occurred in the surface layer of the model (Fig. 7a). Onshore flow of 5-10 cm sec^{-1} then occurred in the lower layer (Fig. 7b), with maximum upwelling velocities of 9 m day^{-1} found on the inner shelf, and as much as 14 m day^{-1} on the middle shelf. A K_z of 80.9 cm^2 sec^{-1}, computed during the 5-12 April case, at the 44 m isobath would yield an effective mixing velocity of ~16 m day^{-1} to resuspend chlorophyll, if more algal biomass were located in the lower layer than in the middle or upper layers of the water column. In this situation, a combination of the calculated K_z and w, together with an assumed w_s of 20 m day^{-1}, would still allow a vertical input of phytoplankton to the euphotic zone at a net rate of 10 m day^{-1}.

Using a constant sinking velocity of 20 m day^{-1} and the time-dependent growth and grazing rates [case (c) of Table 1], we will describe the seasonal change in biological response to three such downwelling cases on 3 March, 4 April, and 16 April, and three upwelling cases on 16 March, 11 April, and 20 April 1979. At the beginning of March, for example, the incident radiation in the mid-Atlantic Bight was <250 g cal cm^{-2} day^{-1}, which, over a well-mixed water column, would yield a mean <u>in situ</u> light intensity of

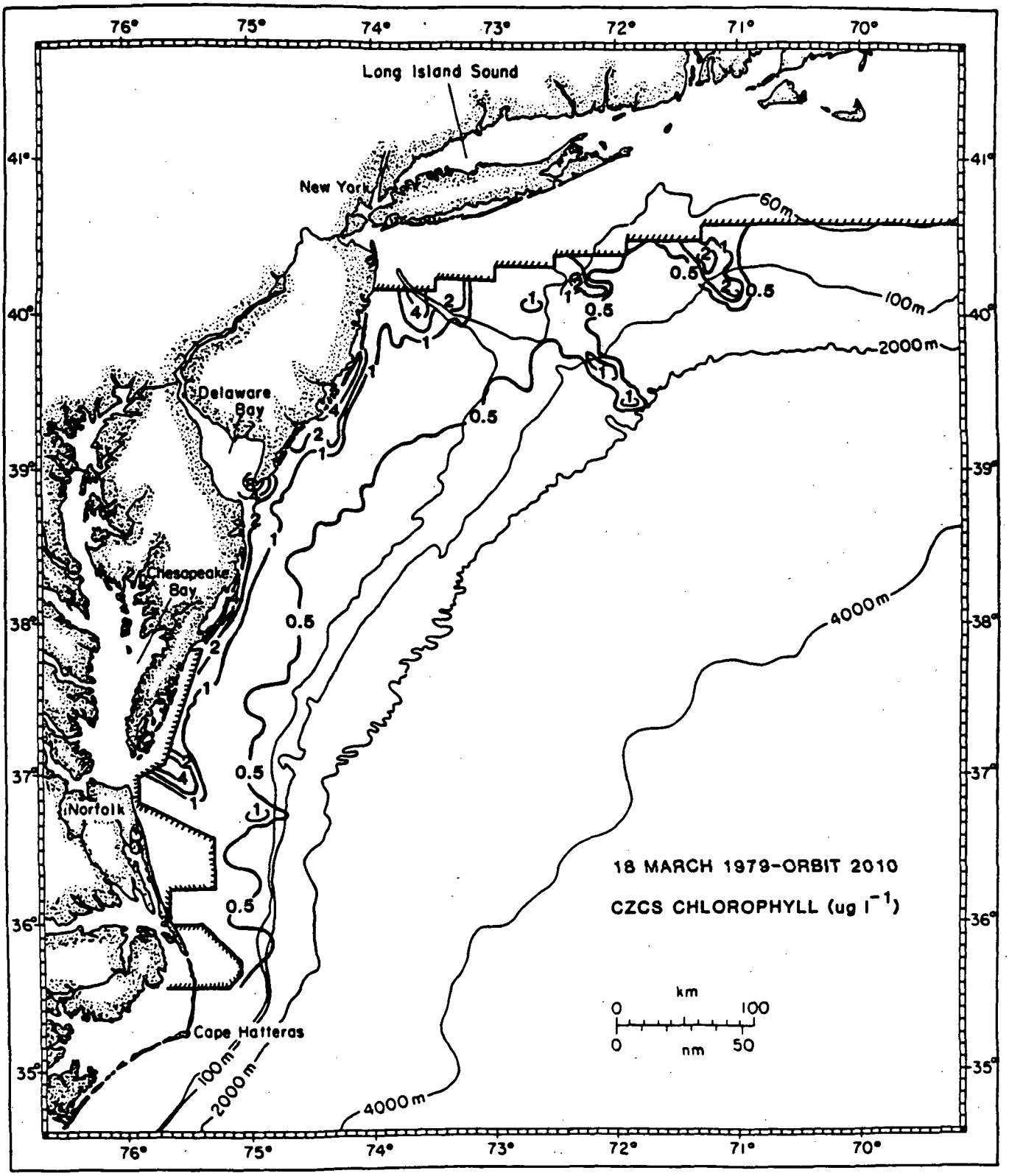

Figure 10. The CZCS estimate of surface chlorophyll during orbit 2010 on 18 March 1979.

respectively 64 and 32 g cal cm^{-2} day^{-1} within the surface layers of the model at the 30 and 60 m isobaths (Fig. 4). Below an in situ light intensity of 40 g cal cm^{-2} day^{-1}, the spring bloom does not occur at these latitudes (RILEY, 1967; HITCHCOCK and SMAYDA, 1977).

Consequently, under a weak northeast wind forcing of 0.21 dynes cm^{-2} from 088°T through 4 March 1979 (Fig. 5), the 0.5 and 1.0 µg ℓ^{-1} isopleths of simulated chlorophyll in the surface layer were then located along the 20 m isobath (Fig. 8a). The dashed lines of Figure 8 and subsequent plots are respectively the 10 m, 20 m, 60 m, 100 m, and 200 m isobaths. After 4 days of nearshore growth at this time in the simulation, the 5.5 µg-at ℓ^{-1} isopleth of nitrate of the upper layer was also coincident with the 20 m isobath (Fig. 8b). With a sinking velocity of 20 m day^{-1}, and a maximum nearshore (<30 m depth) downwelling velocity of 11.3 m day^{-1}, 5.0 µg chl ℓ^{-1} were computed in the lower layer near the 20 m isobath (Fig. 8c). The 1 µg ℓ^{-1} isopleth of chlorophyll in the lower layer was instead coincident with the 60 m isobath, while the 0.5 µg ℓ^{-1} isopleth was found at the 100 m isobath, ~50-100 km farther seaward than those of the upper layer. At a grazing loss of only about 10% of the daily primary production, most of this nearshore algal biomass of the model was not consumed in early March, but advected downstream and seaward.

By the northwest wind forcing of 0.90 dynes cm^{-2} from 287°T on 16 March 1979, the 2.5 µg ℓ^{-1} isopleth of chlorophyll in the lower layer had begun to impinge on the 60 m isobath as well (Fig. 9c). More than 10 µg chl ℓ^{-1} was found in the lower layer of the model at the 20 m isobath (Fig. 9c), similar to shipboard observations during

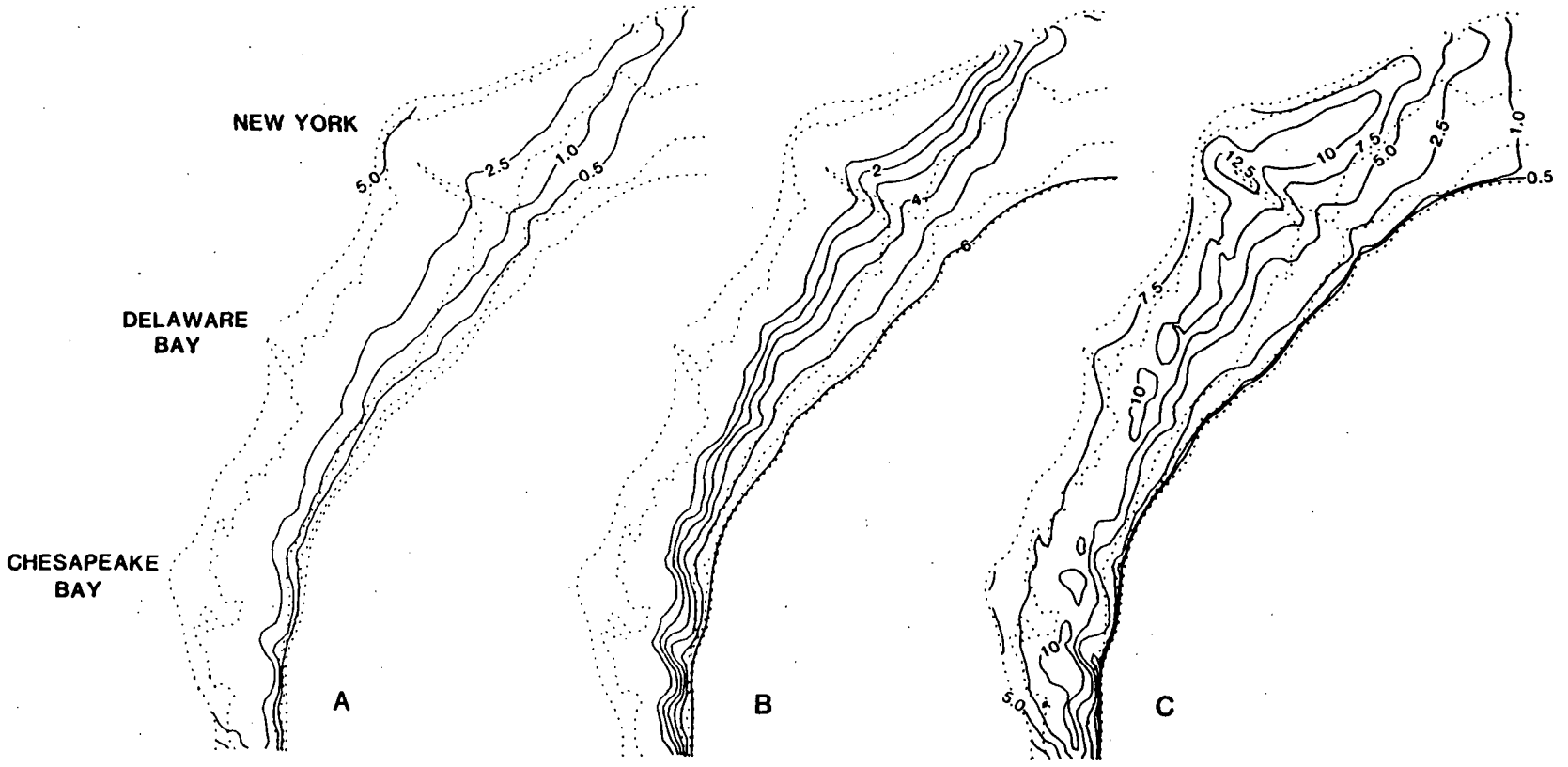

Figure 11. The simulated chlorophyll (μg ℓ^{-1}) of case (c) within the upper a) and lower c) layers, as well as nitrate (μg-at ℓ^{-1}) in b) the upper layer, on 4 April 1979.

24 March 1979 (WALSH et al., 1987a). With this upwelling circulation of 10-14 m day^{-1} and a strong mixing coefficient of 74.2 cm^2 sec^{-1}, the 0.5 μg ℓ^{-1} isopleth of surface chlorophyll occurred at the 60 m isobath (Fig. 9a), similar to the spatial pattern detected on 18 March 1979 during CZCS orbit 2010 (Fig. 10). After two weeks of growth in the model, the nearshore dissolved nitrogen stocks were depleted, with the 1 μg-at ℓ^{-1} isopleth of surface nitrate found at the 20 m isobath, and the 5.5 μg-at ℓ^{-1} isopleth at the 60 m isobath (Fig. 9b). Subsequent generations of phytoplankton within shallow waters (<20 m depth) would now grow in the model under nutrient limitation, since the ambient nitrate concentrations here were less than the half-saturation constant -- recall eq. (13).

After a month of increasing solar radiation, the in situ light intensity within the upper 30 m at the 90 m isobath was >40 g cal cm^{-2} in early April, while the nitrate concentration was still 5.5 μg-at NO_3 ℓ^{-1} here (Fig. 11b). The daily grazing stress was now about 20% of the outer shelf production, however, and as much as 50% of the inner shelf production. Within another downwelling circulation on 4 April, i.e., analogous to 3 March, a uniform algal biomass of >3 μg chl ℓ^{-1} occurred in surface waters, landward of the 50 m isobath (Fig. 11a).

Within the lower layer of the model, which reflects the history of the surface primary production, a mid-shelf maximum of >10 μg chl ℓ^{-1} instead occurred between the 20-60 m isobaths on 4 April (Fig. 11c). With less than 0.5 μg-at NO_3 ℓ^{-1} found landward of the 20 m isobath, except for the estuarine discharge, the dissolved source

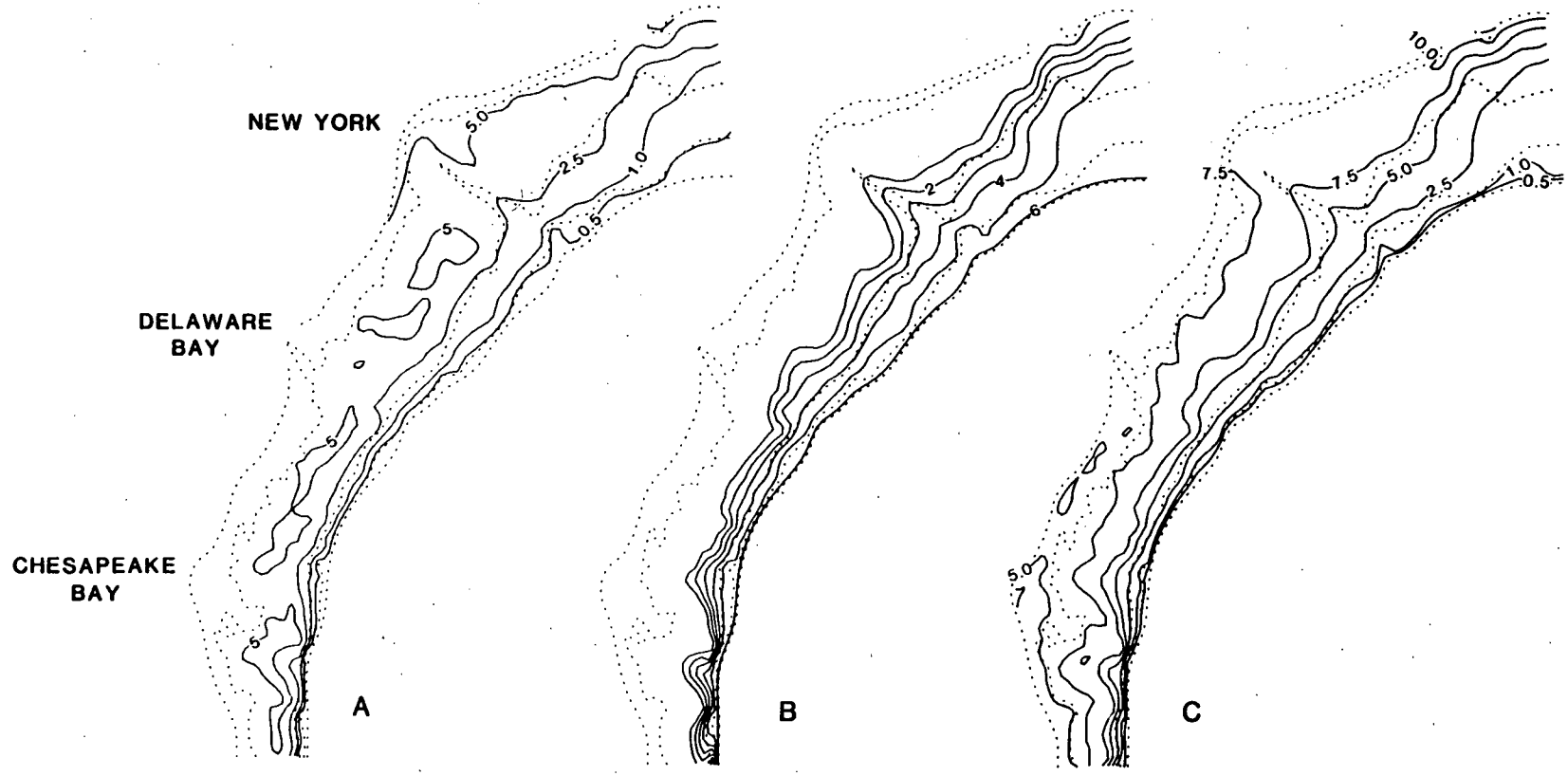

Figure 12. The same variables 7 days later on 11 April 1979.

of particulate nitrogen, sinking out of the surface to nearshore bottom waters, had been curtailed by this time in the spring bloom. The mid-shelf maximum of the model on 4 April 1979 was also the result of prior offshore advection of uneaten phytoplankton from shallow waters. A near-bottom maximum of >20 μg chl ℓ^{-1} was found at mid-shelf on the 50-60 m isobaths during a 1-5 April 1984 cruise (WALSH et al., 1987b).

A strong upwelling circulation of 9-14 m day^{-1} by 11 April 1979 (Fig. 7) led to a simulated resuspension of chlorophyll from this bottom layer (Fig. 12c) to the top layer (Fig. 12a) at mid-shelf off New Jersey to Virginia, and immediately south of Long Island. The lower layer of the model was depleted of chlorophyll, while the upper layer was enhanced. Thus in situ growth within the euphotic zone may not have accounted for all of the surface increment of chlorophyll, calculated at mid-shelf between April 4 and 11 (Fig. 12a).

Similar mid-shelf maxima of surface algal biomass (Fig. 11a) had been detected aboard ship in April 1975 (WALSH et al., 1978) and during orbit 2452 of the CZCS on 19 April 1979 (WALSH et al., 1987a). Although nutrient-rich water was advected shoreward within the aphotic zone (Fig. 7) in response to upwelling favorable winds (Fig. 5), the nitrate content of the upper layer at mid-shelf was actually reduced by ~1 μg-at NO_3 ℓ^{-1} between April 4 (Fig. 11b) and 11 (Fig. 12b). At a nitrate/chlorophyll ratio of 0.5, about 40-50% of the primary production, i.e., biomass increment + grazing loss, was the result of particulate incorporation of dissolved nitrate.

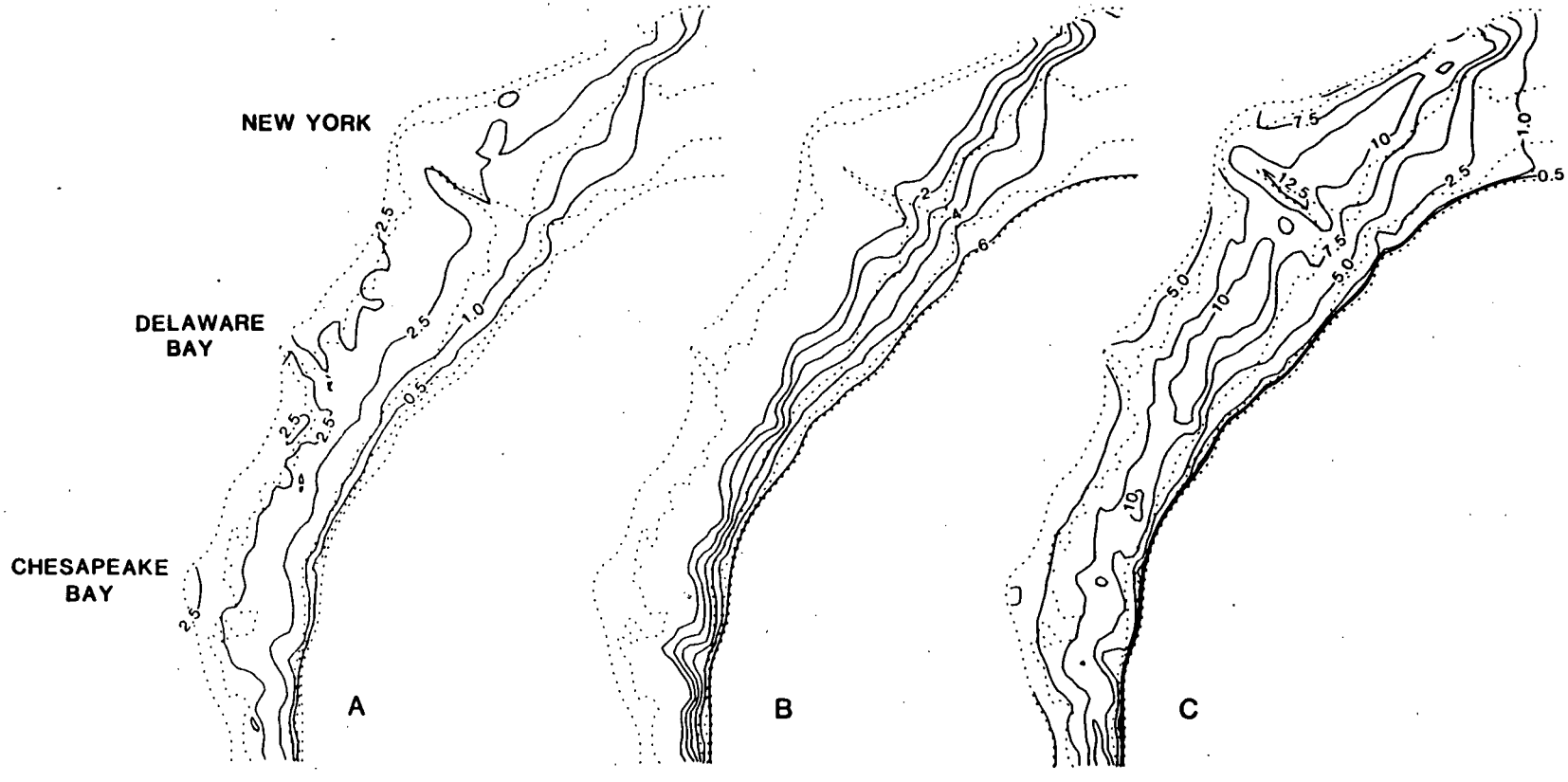

Figure 13. The same variables 12 days later on 16 April 1979.

Another reversal of the winds from the northeast yielded the third downwelling case of the model by 16 April 1979, with a K_z of only 31.2 cm^2 sec^{-1}, but a maximum downward entrainment velocity of 22-30 m day^{-1}. High chlorophyll (>10 μg ℓ^{-1}) was again found within the bottom layer south of Long Island and at mid-shelf, from New Jersey to Delaware (Fig. 13c). In contrast to the second downwelling case of 4 April (Fig. 11a), however, a mid-shelf maximum of 2.5 μg chl ℓ^{-1} was simulated by 16 April in the surface layer of the model (Fig. 13a), with plumes of chlorophyll extending off the Hudson and Delaware estuaries. These were also observed by the CZCS during orbit 2425 on 17 April 1979 (Fig. 14). Perhaps as a result of an apparent lack of surface export of chlorophyll from the Chesapeake estuary (Fig. 13a), the chlorophyll content of the model's lower layer at mid-shelf off Virginia on 16 April (Fig. 13c) was less than that on 4 April (Fig. 11c).

The third upwelling case, of 0.58 dynes cm^{-2} on 20 April 1979 from 341°T, was the weakest northwest wind forcing, with maximum positive vertical velocities in the model of only 6-13 m day^{-1}, and a K_z of 35 cm^2 sec^{-1}. At the 44 m isobath, such an upwelling rate of 6 m day^{-1} and an effective mixing rate of only 7 m day^{-1} would actually result in a net downward algal transfer of 7 m day^{-1}, with the assumed sinking rate of 20 m day^{-1}. The simulated surface nitrate pattern on 20 April (Fig. 15b) was quite similar to both the previous upwelling event on 11 April (Fig. 12b) and the preceding downwelling case on 16 April (Fig. 13b), indicating little flux of nitrate to the euphotic zone.

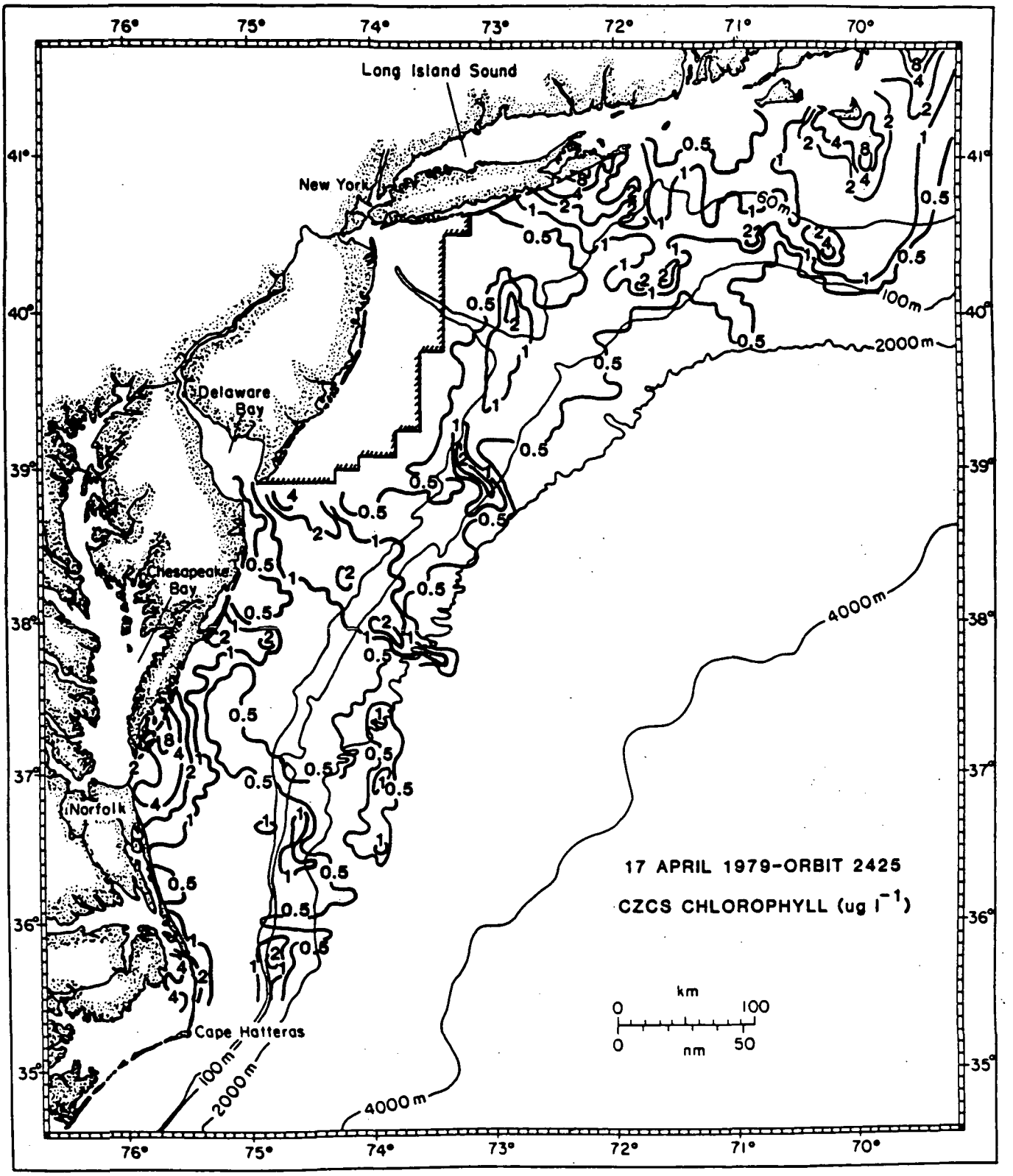

Figure 14. The CZCS estimate of surface chlorophyll during orbit 2425 on 17 April 1979.

A chlorophyll plume of >2.5 μg ℓ^{-1}, derived from the Hudson River export, was found in the upper layer of the model off New York (Fig. 15a), with local maxima of the same amount of algal biomass found at mid-shelf, farther to the south. The higher biomass simulated previously by the model in the second upwelling case on 11 April (Fig. 12a) and observed by the CZCS during orbit 2452 on 19 April 1979 (WALSH et al., 1987a), was not reproduced by this version of the model. Part of the chlorophyll increase detected by the CZCS on 19 April may have been the result of surface export of macrophytes from coastal marshes, rather than just resuspension of near-bottom phytoplankton residues. A lower algal sinking rate of 1 m day^{-1} in the model would have yielded a bloom, of course, in this region of the shelf.

Over the 58-day period of this particular simulation of the 1979 spring bloom, the phytoplankton export was a mean, over 325 km long segments at the shelf-break, of 1.30 g chl m^{-2} day^{-1} between Long Island and New Jersey, 2.25 g chl m^{-2} day^{-1} between New Jersey and Maryland, and 3.64 g chl m^{-2} day^{-1} between Maryland and Cape Hatteras (Fig. 4). More than 90% of this export occurred in the lower layer of the model, as indicated by the time history of simulated algal biomass at the 80 m isobath, south of Long Island (Fig. 16). This grid point of the model was adjacent to 1984 fluorometer moorings at the 80 and 120 m isobaths (WALSH et al., 1987b), which exhibited similar records of chlorophyll fluctuations at depths of 13 m and 75-81 m (Fig. 17). Note that near-bottom chlorophyll concentrations of >2 μg chl ℓ^{-1} were found after Julian day 80 in both the simulated (Fig. 16) and observed (Fig. 17) time series.

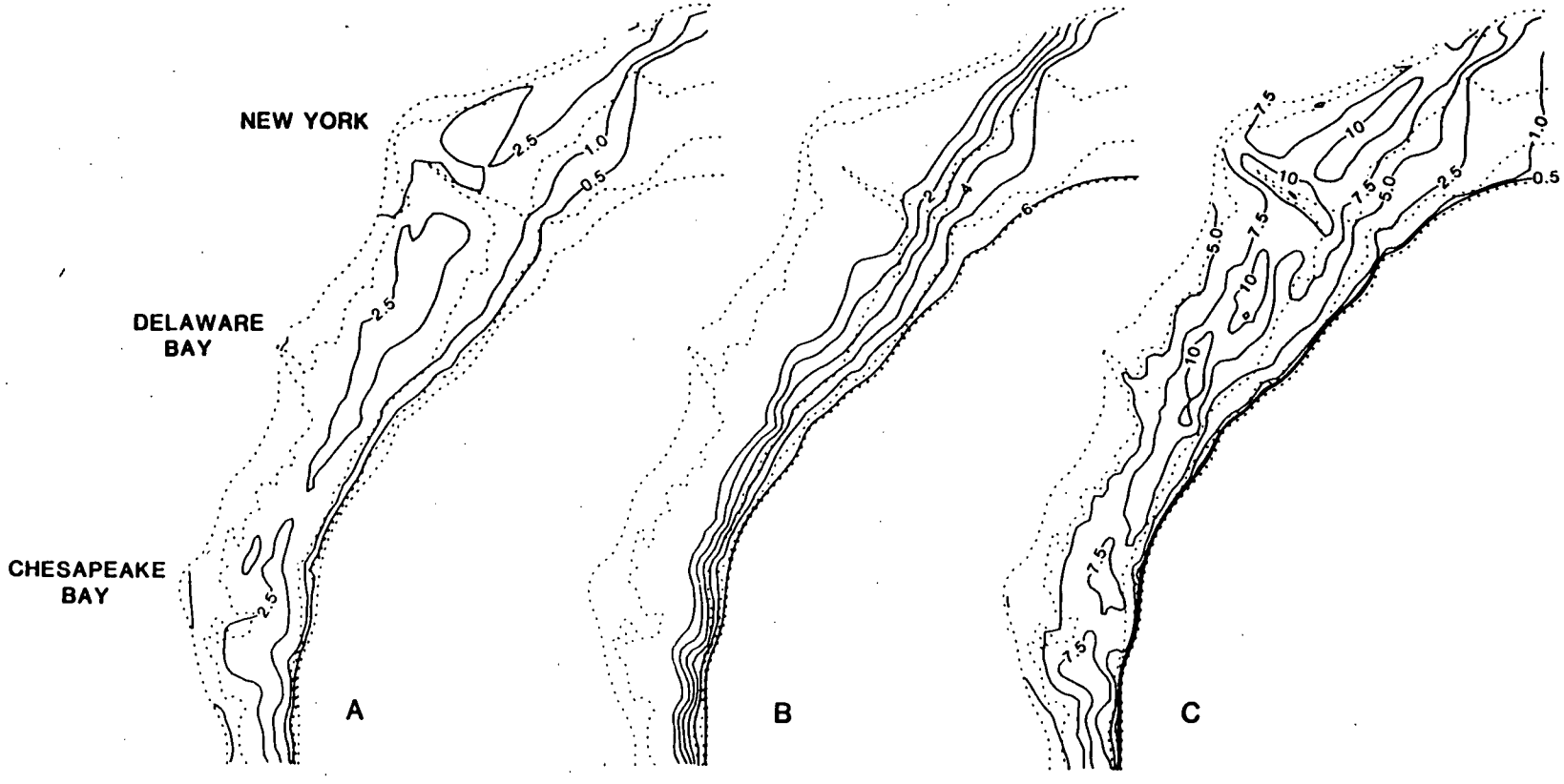

Figure 15. The simulated chlorophyll (μg ℓ^{-1}) of case (c) within the upper a) and lower c) layers, as well as nitrate (μg-at ℓ^{-1}) in b) the upper layer, on 20 April 1979.

The ability of this case of our simulation model to replicate both spatial patterns of chlorophyll detected by the CZCS (Figs. 10, 14), and temporal patterns detected by moored fluorometers (Fig. 17), suggests that a simulated export of 2.40 g chl m^{-2} day^{-1} may be a reasonable time-averaged mean for March-April in the mid-Atlantic Bight. If we assume that this export occurred at the 120 m isobath, with 90% in the lower third of the water column, the depth-averaged mean over the whole water column would then be 0.88 g chl m^{-2} day^{-1}. The possible range and implication of such an estimate is discussed in relation to our evaluation of the parameter space of the model.

DISCUSSION

Nine separate cases of this simulation model were run (Table 1), with, for example, sinking rates of 1 m day^{-1} (a), 10 m day^{-1} (b), and 20 m day^{-1} (c), at an exponential grazing rate, at the normal mixing rate, and at the normal estuarine or upstream boundary conditions. The above results were from case (c). In another run, the mixing rate was doubled (d), with a sinking rate of 1 m day^{-1}, and the rest of the parameters unchanged. In a third experiment, the zooplankton grazing rate was assumed to be zero (e), or to vary linearly with time (f) rather than as an exponential function, at an intermediate sinking rate of 10 m day^{-1}, with the normal mixing rate and boundary conditions. A fourth experiment increased tenfold the estuarine input of dissolved nitrogen, at upstream boundary conditions of 6 μg-at NO_3 ℓ^{-1} (g) and 1 μg-at NO_3 ℓ^{-1} (h), with a sinking rate of 20 m day^{-1}, an exponential grazing rate, and the normal mixing rate. Finally, the

Table 1. *Parameter evaluation of the 1979 spring bloom simulation*

Experiment	Sinking Rate[1]	Mixing Rate	Grazing Rate	Estuarine Boundary	Upstream Boundary	Primary Production[2]	Grazing Loss[2]	Shelf Export[3]	Slope Export[3]
a	1	1x	Exp	1x	1x	10.4	6.9	21.5	1.6
b	10	1x	Exp	1x	1x	8.2	5.1	20.0	1.1
c	20	1x	Exp	1x	1x	6.8	3.9	18.9	0.9
d	1	2x	Exp	1x	1x	10.2	6.8	21.6	1.5
e	10	1x	None	1x	1x	10.0	-0-	39.5	2.7
f	10	1x	Linear	1x	1x	4.7	5.1	7.5	0.2
g	20	1x	Exp	10x	1x	7.2	4.1	19.2	0.9
h	20	1x	Exp	10x	0.17x	6.3	3.8	19.2	0.8
i	20	1x	Exp	1x	0.17x	6.4	3.5	18.9	0.8

[1] $m\ day^{-1}$

[2] $mg\ chl\ m^{-2}\ day^{-1}$

[3] $g\ chl\ m^{-2}\ day^{-1}$

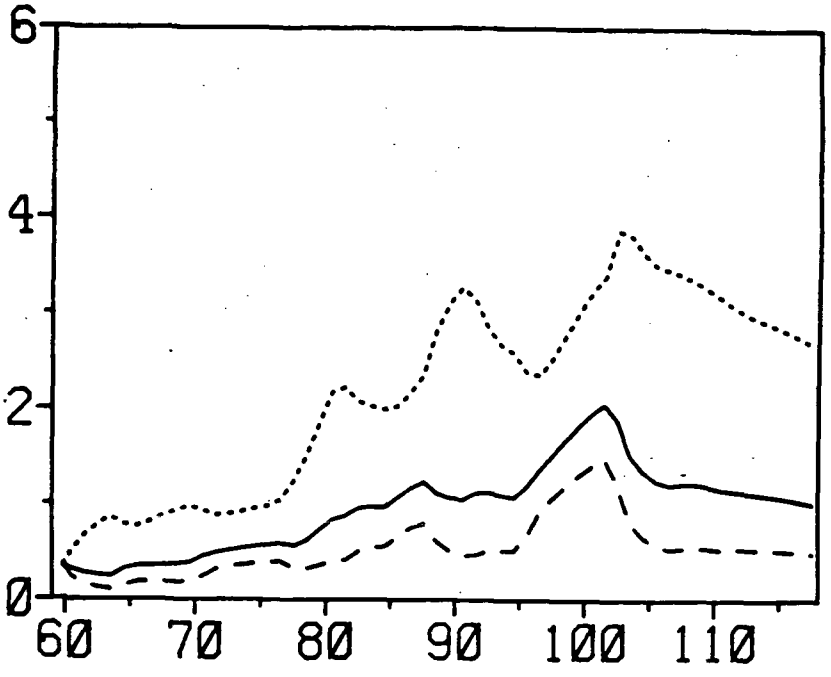

Figure 16. The simulated chlorophyll content ($\mu g\ \ell^{-1}$) at noon of each Julian day from 1 March to 27 April 1979 within the upper (--), middle (—), and lower (...) layers of the 80 m water column at a grid point, adjacent to the 1984 fluorometer moorings, south of Long Island.

last experiment considered an upstream boundary condition of only 1 μg-at NO_3 ℓ^{-1} (i), at the normal estuarine flux of nitrogen, the usual mixing rate, a sinking rate of 20 m day^{-1}, and an exponential grazing rate.

With a surface area of the model of 8.52 x 10^{10} m^2, an upstream shelf boundary area of 8.95 x 10^6 m^2, a downstream shelf boundary area of 2.10 x 10^6 m^2, a shelf-break boundary area of 8.85 x 10^7 m^2, and an estuarine boundary area of 2.54 x 10^6 m^2, the units of Table 1 can be converted to total mass fluxes. For example, a mean of 8.9 x 10^8 g chl day^{-1} was produced over all of the mid-Atlantic shelf during March-April 1979 for case (a) with a sinking rate of 1 m day^{-1}. An average of 66% of this synthesized chlorophyll was lost each day to grazing, while 21% was lost to export, either downshelf or within slope waters. The remaining 13% had not yet been removed from the shelf water column by the end of the simulation (Table 1). In case (e) of no grazing loss (Table 1), 38% of the March-April daily chlorophyll production was instead lost as physical export past the shelf and slope boundaries (Fig. 4) over the same time period.

Using a C/chl ratio of 45/1 (MALONE et al., 1983), the mean daily fixation of carbon, based just on nitrate, would have been 0.47 g C m^{-2} day^{-1} in case (a) and 0.31 g C m^{-2} day^{-1} in case (c) of the model (Table 1). Averaging over upwelling and downwelling wind events, a mean primary production of 0.57 g C m^{-2} day^{-1} was actually measured in the mid-Atlantic Bight (O'REILLY and BUSCH, 1984) during March-April 1977-80 at 66 stations, excluding the observations from the mouths of the estuaries (WALSH et al., 1987a). Approximately 50% of the spring

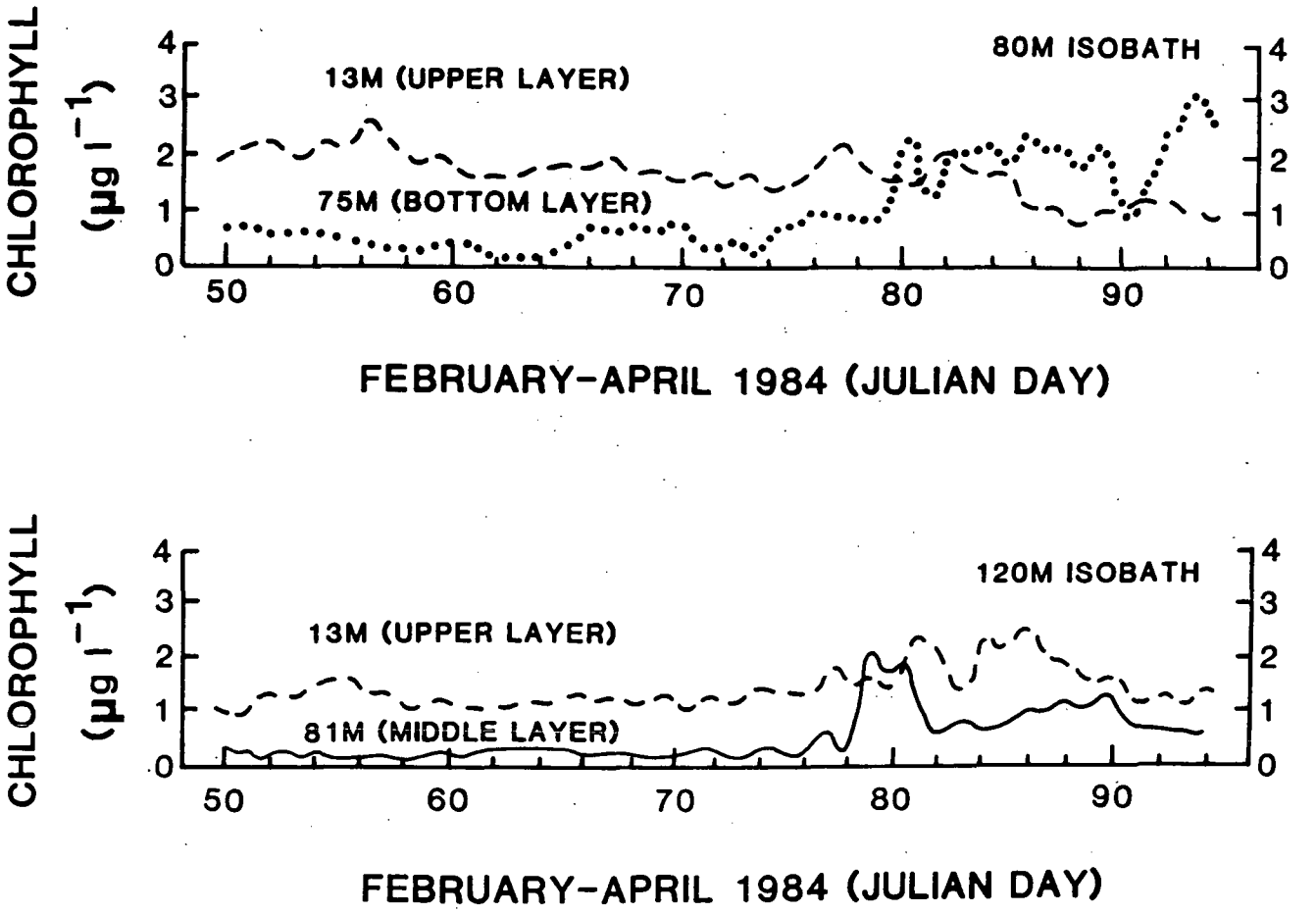

Figure 17. The observed chlorophyll content (μg ℓ^{-1}), after application of a 40-hr low-pass filter, from moored fluorometers both at a) 13 m and 75 m on the 80 m isobath, and at b) 13 m and 81 m on the 120 m isobath, south of Long Island from 19 February to 4 April 1984.

bloom's nitrogen demand is met by nitrate off New York (CONWAY and WHITLEDGE, 1979). The total carbon fixation predicted by the model would thus have been 0.94 g C m^{-2} day^{-1} in case (a) and 0.62 g C m^{-2} day^{-1} in case (c), if uptake of recycled nitrogen had been added to eq. (12).

The productivity difference between these two cases of the model was the result of increased light limitation, induced by changing the sinking rate from 1 m day^{-1} to 20 m day^{-1} (Table 1) i.e., thereby decreasing the residence time of an algal cell within the euphotic zone. In contrast, a doubling of K_z in case (d) had little impact on the production or export of chlorophyll, compared to case (a) in Table 1. The vertical structure of chlorophyll in cases (a) or (d) was quite different, however, from case (c), either over time at the 30 m (Fig. 18) and 50 m (Fig. 19) isobaths, south of Delaware, or within specific spatial patterns in the downwelling (Fig. 20) and upwelling (Fig. 21) circulation modes.

A sinking rate of 1 m day^{-1} allowed no vertical structure of chlorophyll to develop at the 30 m (Fig. 18a) and 50 m (Fig. 19a) isobaths, adjacent to the Philadelphia dump site at 38°37'N, 74°22'W, i.e., east of the mouth of Delaware Bay. A uniform 5-6 μg chl ℓ^{-1} was then found throughout the whole mid-shelf region within either the lower layer of a downwelling circulation on 4 April 1979 (Fig. 20a), or in the surface layer during an upwelling event on 11 April 1979 (Fig. 21a), i.e., Julian days 94-106 of Figure 19a. In cases (a) or (d), the seasonal peak of vertically homogeneous chlorophyll on day 95 at the 50 m isobath (Fig. 19a) followed about two weeks after the

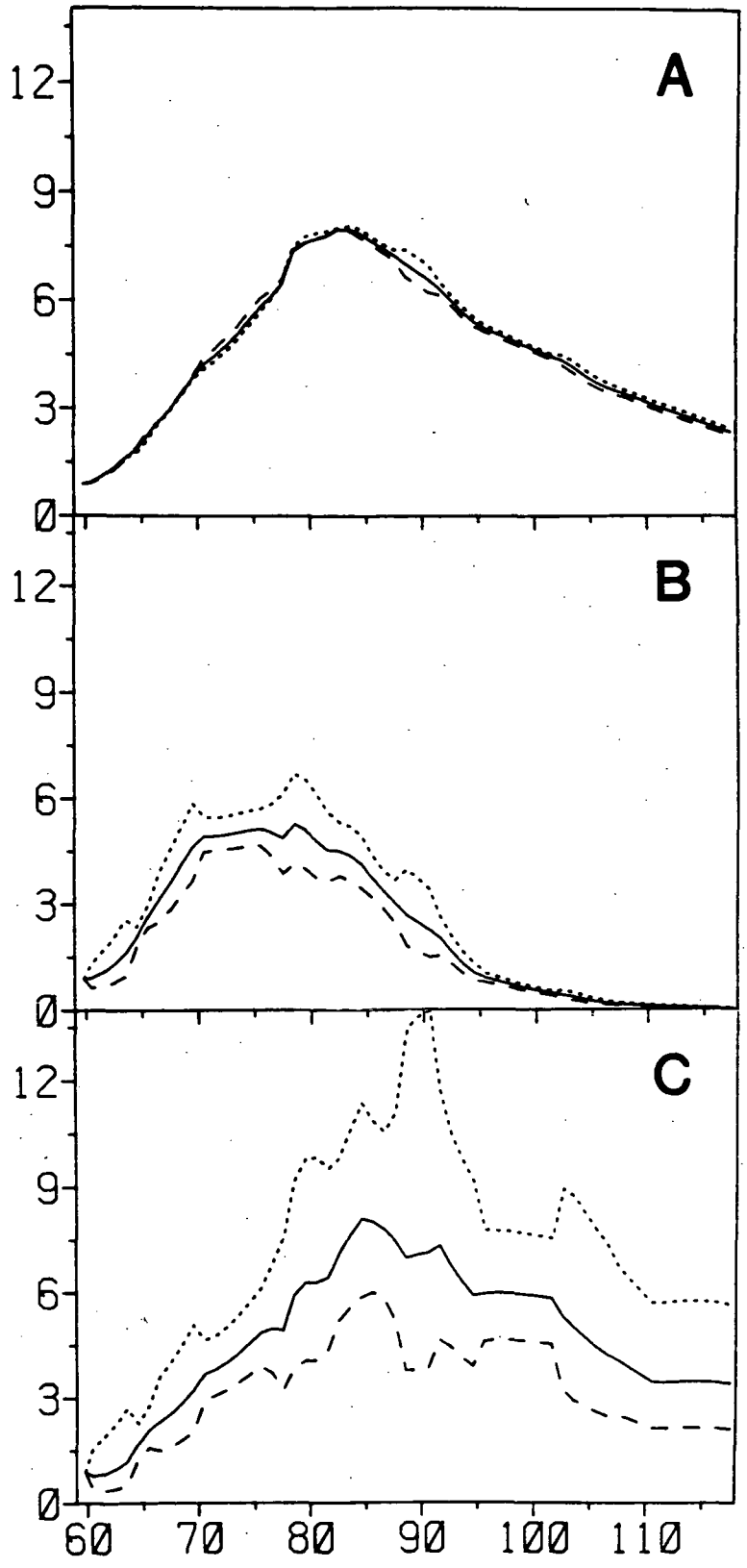

Figure 18. The simulated chlorophyll content (μg ℓ^{-1}) at noon of each Julian day from 1 March to 27 April 1979 within the upper (--), middle (—), and lower (...) layers of the 30 m water column at a grid point, east of Delaware Bay, of a) case (a), b) case (f), and c) case (g).

maximum algal biomass on day 82 at the 30 m isobath (Fig. 18a), i.e., a seaward progression of ~2 km day^{-1}.

In cases (a) or (d), a peak of 6 μg chl ℓ^{-1} throughout the water column was subsequently observed one week later on Julian day 102 at the 80 m isobath, south of Long Island, as well. This was in contrast to about 4 μg chl ℓ^{-1} in the lower layer and 1 μg chl ℓ^{-1} in the upper layer of case (c) -- recall Figure 16. Since high values of 6 μg chl ℓ^{-1} were not found during April from this region, either in the 1984 moored fluorometer records (Fig. 17), or within a previous 9-yr data base of ~5000 stations (Fig. 22), the loss terms of sinking and grazing within cases (a) and (d) were probably too small.

An increased sinking rate of 10 m day^{-1} and no grazing loss of case (e) resulted (Table 1) in the same primary production as cases (a) and (d). The average April chlorophyll of the lower layer in case (e) was 11.42 μg ℓ^{-1} (Table 2), however, about 3-fold that of cases (a) or (d). The average daily algal export to the slope of the lower layer of the model past the location of the fluorometer moorings in case (e) also increased to 4.0 g chl m^{-2} day^{-1}, compared to an observed 1984 mean of 2.7 g chl m^{-2} day^{-1} (WALSH et al., 1987b). The computed slope import of case (e) would actually have been 8.0 g chl m^{-2} day^{-1}, if recycled nitrogen had been included as a nutrient source of this model.

A linear grazing stress, which was larger than the exponential formulation, and the same 10 m day^{-1} sinking rate of case (f), instead consumed all of the March-April primary production on a mean basis (Table 1). The algal biomass above the 30 m (Fig. 18b) and 50 m

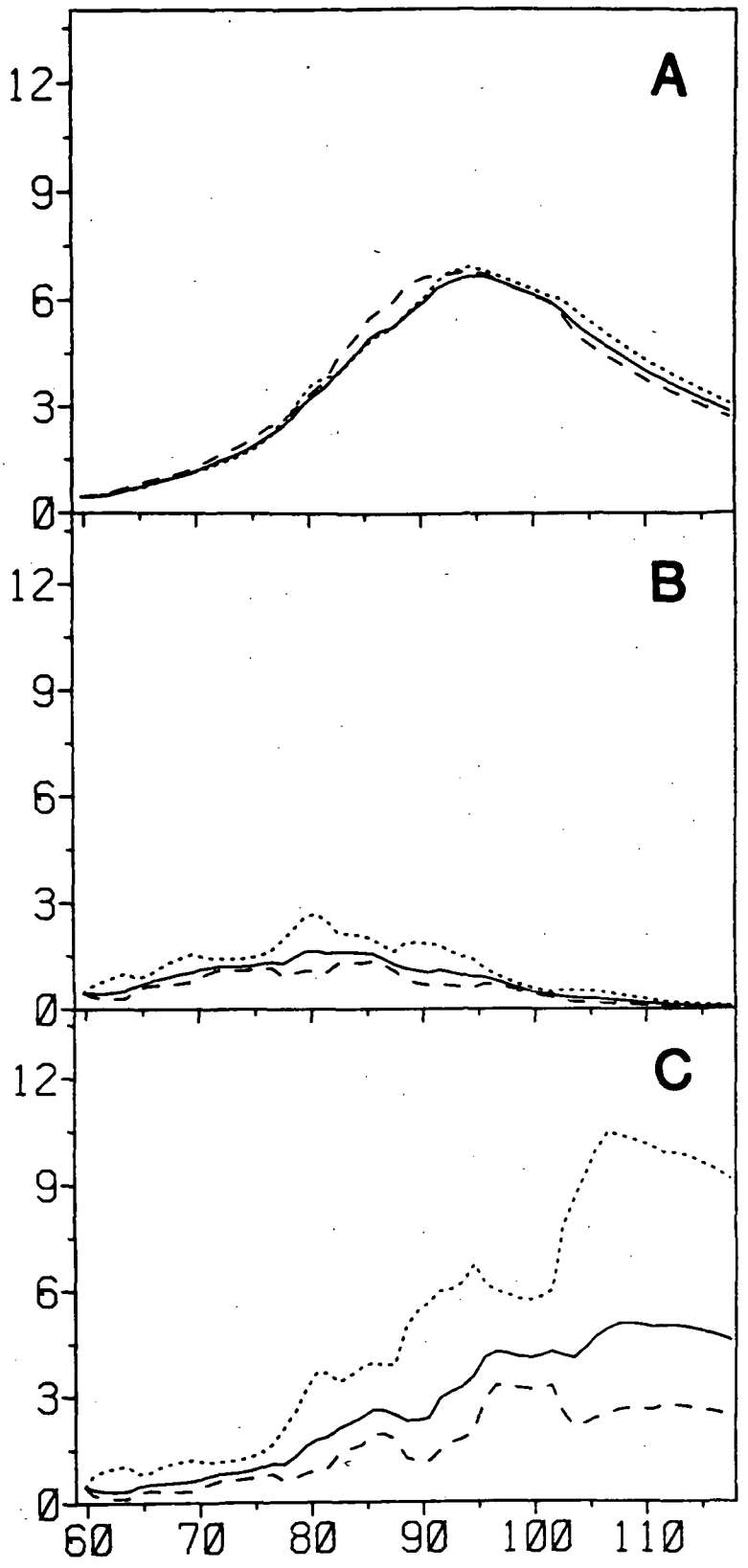

Figure 19. The simulated chlorophyll content (μg ℓ^{-1}) at noon of each Julian day from 1 March to 27 April 1979 within the upper (--), middle (—), and lower (...) layers of the 48 m water column at a grid point, adjacent to the Philadelphia dumpsite east of Delaware Bay, of a) case (a), b) case (f), and c) case (g).

(Fig. 19b) isobaths was reduced to zero by Julian day 115 of case (f), with only 0.5-1.0 μg chl ℓ^{-1} found previously on 4 April (20b) and 11 April (21b) 1979. The average 1979 March-April export at the 80 m isobath of this third grazing experiment in case (f) was only 0.3 g chl m^{-2} day^{-1}, an order of magnitude less than the observed flux in 1984.

The exponential grazing stress and the 20 m day^{-1} sinking rate of case (c) thus appeared to be the best combination of loss terms of this simulation model to approximate prior satellite (Figs. 10, 14), moored fluorometer (Fig. 17), and shipboard (Fig. 21) estimates of chlorophyll. We accordingly used these parameters of the model to evaluate changes of the boundary fluxes of nutrients within cases (g), (h), and (i). The lingering 5 μg-at ℓ^{-1} concentration of nitrate across the shelf, south of Martha's Vineyard, in Figure 11b, for example, was an artifact of the time invariant upstream boundary condition of 6 μg-at NO_3 ℓ^{-1} in case (c). A reduction of the upstream boundary condition to 1 μg-at NO_3 ℓ^{-1} (Table 1) in cases (h) and (i) did not significantly alter the primary production, grazing loss, or export, however, compared to case (c), and we discuss instead the results of the eutrophication case (g).

A tenfold increment of the estuarine nutrient loading to the mid-Atlantic Bight in case (g) significantly increased the nearshore chlorophyll concentrations of the upper (Fig. 21c) and lower (Fig. 20c) layers between Cape May and Montauk Point, i.e., the New York Bight, as well as off Delaware Bay, and off Chesapeake Bay, compared to the previous results of case (c) in Figures 11c and 12a.

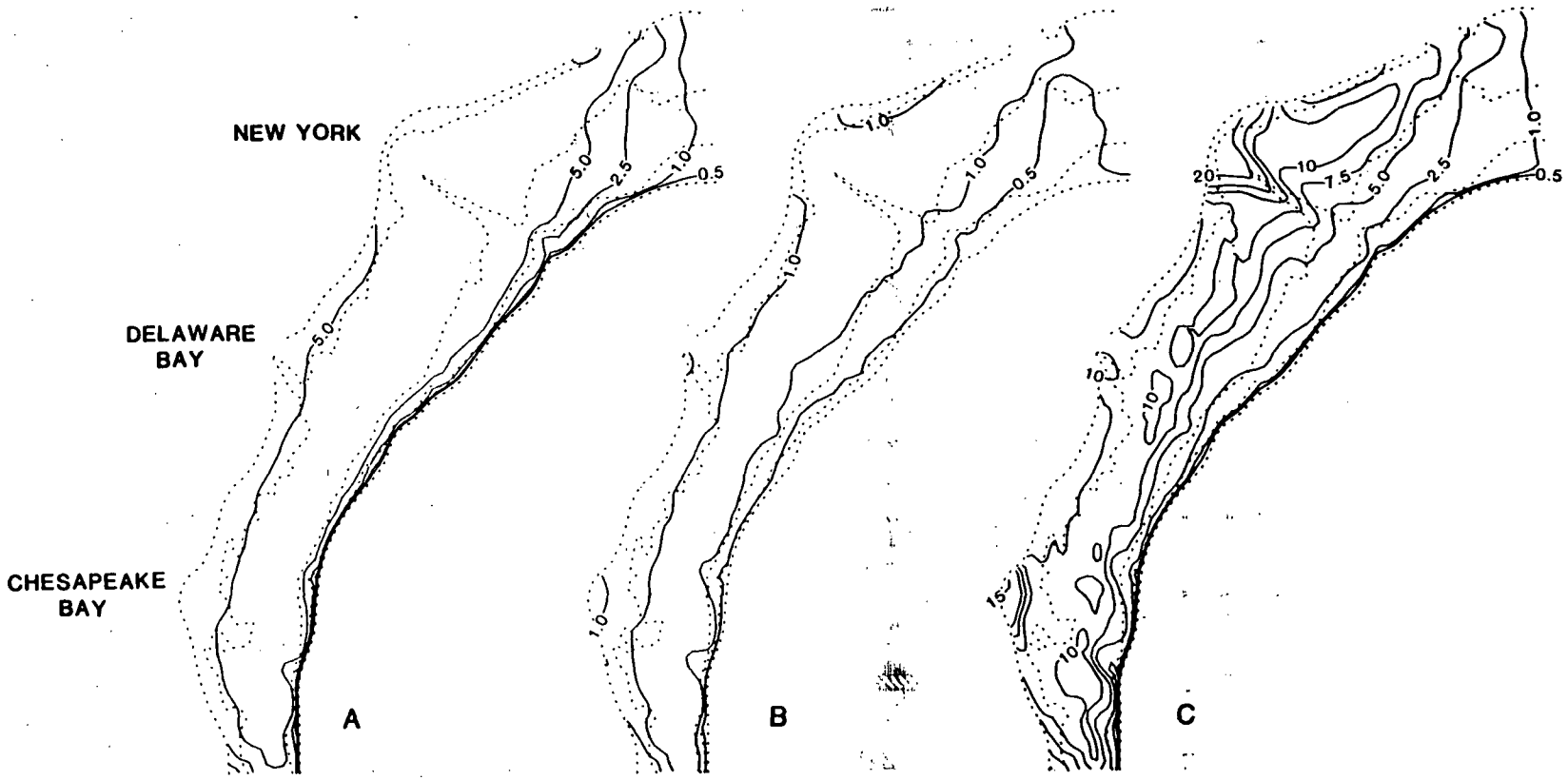

Figure 20. The simulated chlorophyll (μg ℓ^{-1}) within the lower layer of a) case (a), b) case (f), and c) case (g) on 4 April 1979.

The algal biomass of case (g) did not increase much either at the 30 m (Fig. 18c) and 50 m (Fig. 19c) isobaths off Delaware, however, or within the whole spatial domain of the model (Table 2). The primary production of the entire mid-Atlantic Bight (Table 1) only increased by 5% in case (g).

Since the export of estuarine nitrogen to the shelf in case (g) was still only 10% of that from the upstream boundary, this result is not surprising. It does raise the point, however, that compression of 4×10^7 data points in one single spatio-temporal mean for each entry of Table 1 obscures the spatial and temporal complexity of both this model and the "real world." Table 1, for example, does not indicate for case (c) that either 90% of the simulated slope import occurs in the lower layer of the model, or that the computed slope import off Virginia is 3-fold that off New York.

Furthermore, the shelf export has a time dependency associated with the estuarine source function. Extension of this calculation for case (g) to 20 May 1979, for example, leads to a 25% increase of the shelf export from the lower layer, since not all of the estuarine-derived particulate matter had reached the shelf-break by 20 April 1979 in the model. This effect is demonstrated by the first and second bar graphs of each month in Figure 21, which are the mean chlorophyll concentrations during 1974-82 in the upper 20 m and the lower 20-50 m, or 20-75 m, of the New York Bight, while the third and fourth bar graphs are other chlorophyll means of an independent data set, taken over the larger area of the mid-Atlantic Bight. During March, April, and May, the chlorophyll concentrations of the New York

Table 2. April 1979 algal biomass (μg chl ℓ^{-1}) scenarios

Experiment	Upper layer	Middle layer	Lower layer	Water column
a	4.01	3.78	3.97	3.92
b	2.64	3.40	4.87	3.64
c	1.81	2.90	5.20	3.30
d	3.95	3.80	3.90	3.88
e	6.16	8.07	11.42	8.55
f	0.25	0.33	0.48	0.35
g	1.97	3.12	5.54	3.55
h	1.75	2.77	4.85	3.12
i	1.59	2.54	4.50	2.88

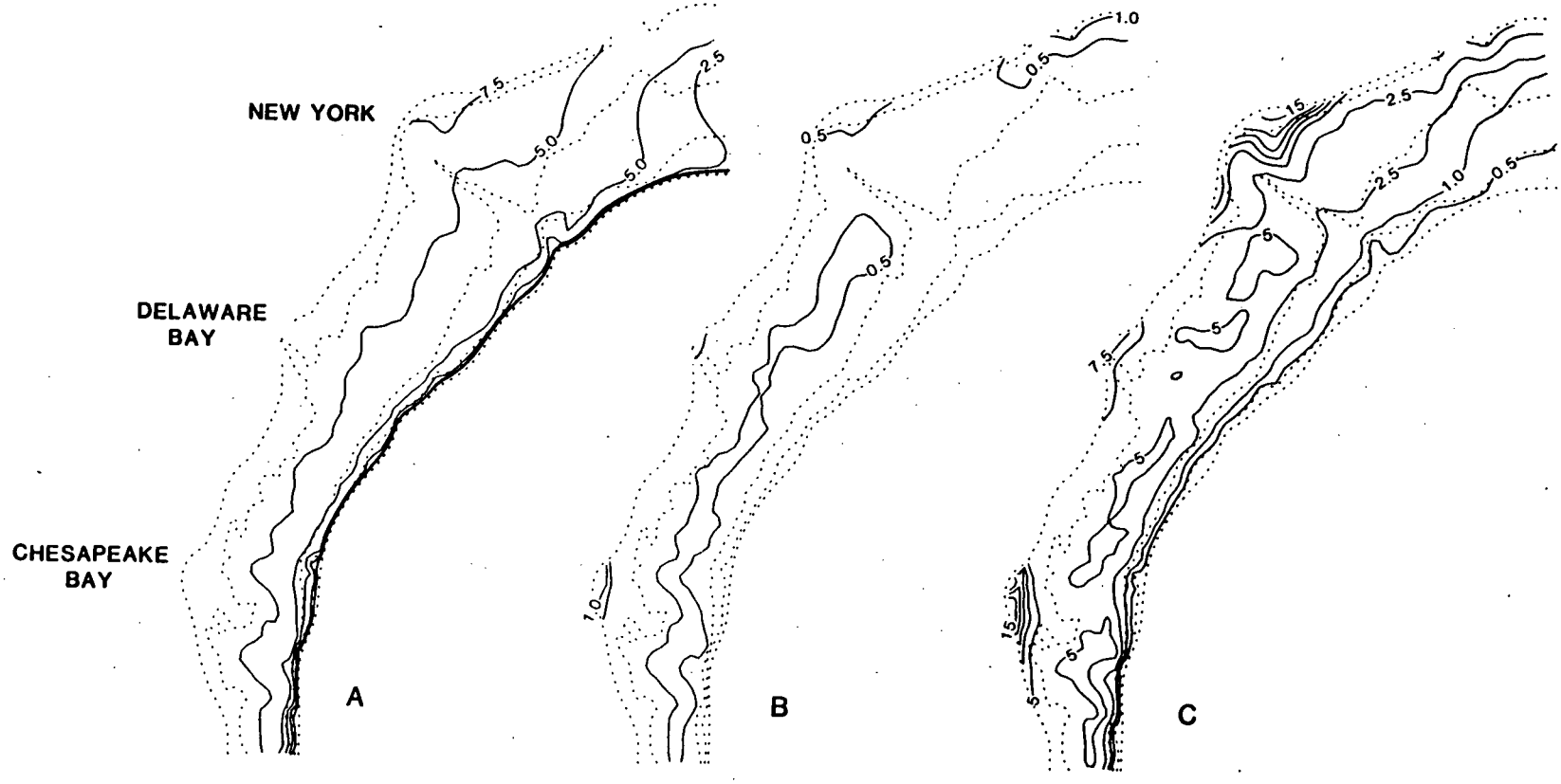

Figure 21. The simulated chlorophyll ($\mu g\ \ell^{-1}$) within the upper layer of a) case (a), b) case (f), and c) case (g) on 11 April 1979.

Bight, from coastal to slope waters, are at least twice that of the whole mid-Atlantic Bight, reflecting the increased nutrient loading of the Hudson River (Fig. 3), i.e., simulated in case (g) as Figures 20c and 21c.

With a decline in nutrient loading from the Hudson River by June (Fig. 3) and a seasonal increase of the grazing stress, there are no differences in mean algal biomass between the data sets of the New York and mid-Atlantic Bights for the months of June to February (Fig. 21). If a grazing stress was not imposed during a simulated tenfold increase of nutrient export from the Hudson River during summer conditions, anoxia, in fact, developed within the New York Bight (STODDARD and WALSH, 1987). Temporal and spatial changes of biochemical processes within the mid-Atlantic Bight are thus both important in determining the fate of primary production within this shelf ecosystem.

The algal biomass left behind in the water column as a net result of the birth and death processes of shelf phytoplankton populations is, by itself, a poor index of the fate of primary production. Averaging over the whole water column, for example, cases (a)-(d) had a range in April algal biomass of only 3.30 to 3.92 μg chl ℓ^{-1} (Table 2), but the surface content of case (c) was less than half that of case (a). The possible twofold increase of April chlorophyll concentrations between 1980 and 1984 (Fig. 1), can thus be simulated (Table 2), with a change in the sinking rate of this simple model (Table 1). Alternatively, the grazing rate in April 1984 might have been less than in April 1980, as indicated by the results of case (e)

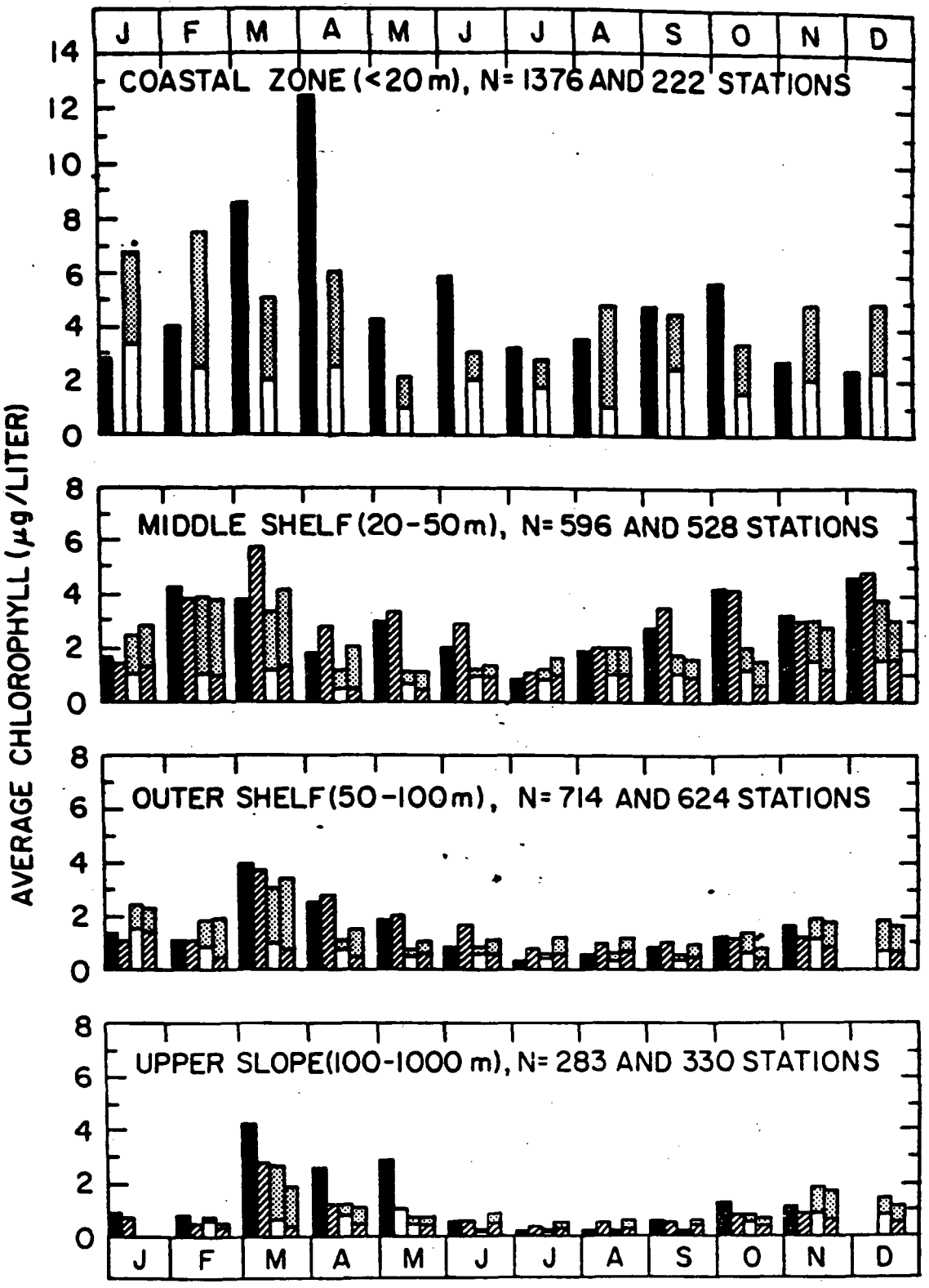

Figure 22. Monthly distribution of mean chlorophyll (µg ℓ^{-1}) within the upper 20 m and the lower 20-50 m, or 20-75 m, of the coastal zone, the middle shelf, the outer shelf, and the slope in the New York Bight (first and second bar graph of each month) and the mid-Atlantic Bight (third and fourth graphs) during 1974-1982 from 4673 stations.

in Table 2. If we had confined the spatial mean of Table 2 to estuarine waters (<20 m) of case (g), moreover, a tenfold increase of the nutrient supply would also have led to more than a doubling of the algal biomass (Figs. 20c and 21c).

The three alternative scenarios of light limitation, nutrient regulation, and grazing stress are thus each capable of inducing a 2-fold change in algal biomass within the mid-Atlantic Bight (Table 2). In concert, these processes can lead to more than a tenfold variation in downstream and offshore shelf export, amounting to a range of 8% to 38% of the mean March-April primary production (Table 1). We are pleased that such a relatively simple biochemical model, coupled to a simple physical model, can both provide insight on the interaction of these different processes and reproduce chlorophyll fields sensed by satellite, shipboard, and in situ instruments.

If recycled nitrogen had been included as a state variable, case (c) would have predicted a mean March-April primary production of 0.62 g C m^{-2} day^{-1} over the whole model domain, with an export of 2.60 g chl m^{-2} day^{-1} from the lower layer of the model off Long Island. Such biological and physical fluxes of organic matter have been measured in the mid-Atlantic Bight as well (WALSH et al., 1987a, b). Additional field experiments will provide a robustness to such simulation models, which will eventually allow us to predict, rather than hindcast, the coastal zone's response to continuing perturbations of eutrophication, overfishing, and climate modification.

ACKNOWLEDGEMENTS

This research was funded by the Department of Energy, the National Aeronautics and Space Administration, and the National Oceanic and Atmospheric Administration. We particularly wish to thank our SEEP colleagues for their arduous efforts at sea during the SEEP-I experiment in 1983-84. In particular, DR. TERRY WHITLEDGE made available nutrient and chlorophyll data for this analysis.

REFERENCES

BANNISTER T. T. (1974) A general theory of steady state phytoplankton growth in a nutrient saturated mixed layer. Limnology and Oceanography, 19, 13-30.

BEARDSLEY R. C., D. C. CHAPMAN, K. H. BRINK, S. R. RAMP, and R. SCHLITZ (1985) The Nantucket Shoals Flux Experiment (NSFE 79). Part I: A basic description of the current and temperature variability. Journal of Physical Oceanography, 15, 713-748.

BODUNGEN B., K. BROCKEL, V. SMETACEK and B. ZEITZSCHEL (1981) Growth and sedimentation of the phytoplankton spring bloom in the Bornholm Sea (Baltic Sea). Kieler Meeresforschung Sonderheft, 5 490-60.

CAPERON J. (1967) Population growth in micro-organisms limited by food supply. Ecology, 48, 715-722.

CARPENTER J. H., D. W. PRITCHARD and R. C. WHALEY (1969) Observations of eutrophication and nutrient cycles in some coastal plain estuaries. In: Eutrophication: Causes, Consequences, and Correctives, National Academy of Science, Washington, pp. 210-224.

CARPENTER E. J. and R. L. GUILLARD (1971) Interspecific differences in nitrate half-saturation constants for three species of marine phytoplankton. Ecology, 52, 183-185.

CHRISTIE, A. M. (1941) N or M? Dodd, Mead & Co., New York, pp. 1-289.

CONWAY H. L. and T. E. WHITLEDGE (1979) Distribution, fluxes, and biological utilization of inorganic nitrogen during a spring bloom in the New York Bight. Journal of Marine Research, 37, 657-668.

CSANADY G. T. (1976) Mean circulation in shallow seas. Journal of Geophysical Research, 81, 5389-5399.

CSANADY G. T. (1981) Shelf circulation cells. Philosophical Transactions of the Royal Society, London, A302, 515-530.

DAGG M. J. and J. T. TURNER (1982) The impact of copepod grazing on the phytoplankton of Georges Bank and the New York Bight. Canadian Journal of Fisheries and Aquatic Science, 39, 979-990.

DECK B. L. (1981) Nutrient-element distributions in the Hudson estuary. Ph.D. Dissertation, Columbia University, pp. 1-396.

EISENSTAT S. C., M. H. SCHULTZ and A. H. SHERMAN (1976) Considerations in the design of software for sparse Gaussian elimination. In: Sparse Matrix Computations, J. R. BUNCH and D. J. ROSE, editors, Academic Press, New York, pp. 1-453.

EPPLEY R. W. and B. J. PETERSON (1980) Particulate organic matter flux and planktonic new production in the deep ocean. Nature, 282, 677-680.

HAN G. C., D. V. HANSEN and J. A. GALT (1980) Steady state diagnostic model of the New York Bight. Journal of Physical Oceanography, 10, 1998-2020.

HITCHCOCK G. L. and T. J. SMAYDA (1977) The importance of light in the initiation of the 1972-1973 winter-spring diatom bloom in Narragansett Bay. Limnology and Oceanography, 22, 126-131.

HOPKINS T. S. and D. A. DIETERLE (1983) An externally forced barotropic circulation model for the New York Bight. Continental Shelf Research, 2, 49-73.

HOPKINS T. S. and L. A. SLATEST (1986) The vertical eddy viscosity and momentum exchange in coastal waters. Journal of Geophysical Research (in press).

HOPKINS T. S. and D. A. DIETERLE (1987) Analysis of the baroclinic circulation in the New York Bight with a 3-d diagnostic model. Continental Shelf Research (in press).

HSUEH Y. (1980) On the theory of deep flow in the Hudson Shelf Valley. Journal of Geophysical Research, 85, 4913-4918.

HSUEH Y and C. Y. PENG (1978) A diagnostic model of continental shelf circulation. Journal of Geophysical Research, 83, 3033-3041.

IKUSHIMA I. (1967) Ecological studies on the productivity of aquatic plant communities, III. Effect of depth on daily photosynthesis in submerged macrophytes. Botanical Annals, Tokyo, 80, 57-67.

JAMART M., D. F. WINTER, K. BANSE, G. C. ANDERSON, and R. K. LAM (1977) A theoretical study of phytoplankton growth and nutrient distribution in the Pacific Ocean off the northwestern U.S. Coast. Deep-Sea Research, 24, 753-773.

MALONE T. C. (1977) Light-saturated photosynthesis by phytoplankton size fractions in the New York Bight, U.S.A. Marine Biology, 42, 281-292.

MALONE, T. C. (1982) Phytoplankton photosynthesis and carbon specific growth: light-saturated rates in a nutrient rich environment. Limnology and Oceanography, 27, 226-235.

MALONE T. C., T. S. HOPKINS, P. G. FALKOWSKI and T. E. WHITLEDGE (1983) Production and transport of phytoplankton biomass over the continental shelf of the New York Bight. Continental Shelf Research, 1, 305-337.

MAYER D. A., G. C. HAN and D. V. HANSEN (1982) The structure of circulation: MESA physical oceanographic studies in New York Bight. Journal of Geophysical Research, 87, 9579-9588.

McCARTHY J. J., W. R. TAYLOR and J. L. TAFT (1977) Nitrogenous nutrition of the plankton in the Chesapeake Bay. Limnology and Oceanography, 22, 996-1011.

NAGLE C. M. (1978) Climatology of Brookhaven National Laboratory, 1974 through 1977. BNL-50857 UC-11, Environmental Control Technical and Earth Science, T10-4500.

NIILER P. P. (1975) Deepening of the wind-mixed layer. Journal of Marine Research, 33, 405-422.

O'REILLY J. E. and D. A. BUSCH (1984) Phytoplankton primary production on the northwestern shelf. Rapports Proceedings-Verbeaux Reunion Conseil pour la Permanent International Exploration de la Mer, 183, 255-268.

RILEY G. A. (1967) The plankton of estuaries. In: Estuaries, G. H. LAUFF, editor, Publication 83, American Association for the Advancement of Science, Washington, pp. 316-326.

ROACHE P. J. (1976) Computational Fluid Dynamics, Hermosa Publications, Albuquerque, pp. 1-446.

SHARP J. H., C. H. CULBERSON and T. M. CHURCH (1982) The chemistry of the Delaware estuary. General considerations. Limnology and Oceanography, 27, 1015-1028.

SMAYDA T. J. (1970) The suspension and sinking of phytoplankton in the sea. Oceanography and Marine Biology Annual Review, 8, 353-414.

SMITH S. L. and P. V. LANE (1987) Grazing of the spring diatom bloom in the New York Bight by the calanoid copepods, Calanus finmarchicus, Metridia lucens, and Centropages typicus. Continental Shelf Research (this volume).

STEELE J. H. (1962) Environmental control of photosynthesis in the sea. Limnology and Oceanography, 7, 137-150.

STODDARD A. and J. J. WALSH (1987) Modeling oxygen depletion in the New York Bight: the water quality impact of a potential increase of waste inputs. In: Urban Wastes in Coastal Environments, D. A. WOLFE, editor, NOAA Professional Paper (in press).

SYSTEMS AND APPLIED SCIENCES CORPORATION (1984) Users guide for the Coastal Zone Color Scanner compressed earth gridded data sets of the northeast coast of the United States for February 28 through May 27, 1979. SASC-T-5-5100-0002-0008-84, 1-15.

WALSH J. J. (1975) A spatial simulation model of the Peru upwelling ecosystem. Deep-Sea Research, 22, 201-236.

WALSH J. J. (1981) Shelf-sea ecosystems. In: Analysis of Marine Ecosystems, A. R. LONGHURST, editor, Academic Press, New York, pp. 159-196.

WALSH, J. J. (1983) Death in the sea: enigmatic phytoplankton losses. Progress in Oceanography, 12, 1-86.

WALSH J. J. (1984) The role of the ocean biota in accelerated ecological cycles: a temporal view. Bioscience, 34, 499-507.

WALSH J. J., T. E. WHITLEDGE, F. W. BARVENIK, C. D. WIRICK, S. O. HOWE, W. E. ESAIAS and J. T. SCOTT (1978) Wind events and food chain dynamics within the New York Bight. Limnology and Oceanography, 23, 659-683.

WALSH J. J., D. A. DIETERLE and W. E. ESAIAS (1987a) Satellite detection of phytoplankton export from the mid-Atlantic Bight during the 1979 spring bloom. Deep-Sea Research (in press).

WALSH J. J., C. D. WIRICK, L. J. PIETRAFESA, T. E. WHITLEDGE, F. E. HOGE and R. N. SWIFT (1987b) High frequency sampling of the 1984 spring bloom within the mid-Atlantic Bight: snyoptic shipboard, aircraft, and in situ perspectives of the SEEP-I experiment. Continental Shelf Research (this volume).

WROBLEWSKI J. S. and J. G. RICHMAN (1986) The nonlinear response of plankton to wind mixing events - implications for larval fish survival. Journal of Plankton Research (in press).